Histology of major organ systems of Nothobranchius fishes: short-lived model species

Authors: Dyková, Iva, Žák, Jakub, Blažek, Radim, Reichard, Martin, Součková, Kamila, et al.

Source: Journal of Vertebrate Biology, 71(21074)

Published By: Institute of Vertebrate Biology, Czech Academy of Sciences

URL: https://doi.org/10.25225/jvb.21074

Journal of Vertebrate Biology

Open Access

J. Vertebr. Biol. 2022, 71: 21074 DOI: 10.25225/jvb.21074

RESEARCH PAPER

Histology of major organ systems of *Nothobranchius* fishes: short-lived model species

Iva DYKOVÁ[1*], Jakub ŽÁK[2], Radim BLAŽEK[1,2], Martin REICHARD[1,2,3], Kamila SOUČKOVÁ[4] and Ondřej SLABÝ[4,5]

[1] *Department of Botany and Zoology, Faculty of Science, Masaryk University, Brno, Czech Republic, e-mail: dykova.iva@gmail.com*

[2] *Institute of Vertebrate Biology, Czech Academy of Sciences, Brno, Czech Republic; e-mail: fish.jakub.zak@gmail.com, blazek@ivb.cz, reichard@ivb.cz*

[3] *Department of Ecology and Vertebrate Zoology, University of Łódź, Łódź, Poland*

[4] *Central European Institute of Technology, Masaryk University, Brno, Czech Republic; e-mail: kamgenet@gmail.com, on.slaby@gmail.com*

[5] *Department of Biology, Faculty of Medicine, Masaryk University, Brno, Czech Republic*

Received 29 November 2021; Accepted 10 January 2022; Published online 21 February 2022

Abstract. A proper understanding of tissue and cell structure is of great importance for correct biological inferences, and particularly so in organisms used as research models. *Nothobranchius* spp. are short-lived freshwater fish species which are promising model organisms for toxicology, evolutionary ecology, aging and regeneration research. Nevertheless, studies examining *Nothobranchius* histology have focused exclusively on a few specific organs and associated functional impairments, and there is a lack of reference material on the natural state and appearance of tissue structure. Here we present a detailed histological map of the major body organ systems, which was built from 300 *Nothobranchius* spp. specimens. This overview offers baseline material for comparative histological studies and provides insights into functional and anatomical aspects of organs related to the unique life cycle of *Nothobranchius* spp.

Key words: short-lived killifish species, tissue structure, cell ultrastructure

Introduction

Histology, the study of microscopic structures of tissues and organs, has developed from a purely descriptive approach into a modern discipline which correlates morphology with the function of structural units of organisms. This field became fundamental to diverse branches of human medicine and animal health, including those focused on fish. The current state of knowledge of fish histology is the result of many years of studies focused in particular on commercially important species, and hence does not encompass the great diversity of teleosts. More information is urgently needed in this field, especially for species with increasing importance in the field of biomedicine and biogerontology. This requirement also applies to fish species that serve as valuable laboratory models for studies of natural and pathological processes.

The introduction of fish into biomedical research has yielded copious new data, particularly due to rapid development of molecular methods. The

* *Corresponding Author*

focus on molecular data in fish model taxa has rendered studies of microscopic structure to be temporarily undervalued (Menke et al. 2011). This outcome applies to zebrafish, *Danio rerio*, a model fish well established for decades (Lieschke & Currie 2007), as well as to emerging model fish species of the genus *Nothobranchius* (Nothobranchiidae) (Cellerino et al. 2016, Hu & Brunet 2018). A review of adult zebrafish anatomy and histology was published only ten years ago (Menke et al. 2011). A comprehensive overview of *Nothobranchius* spp. histology has hitherto been missing, but is addressed in the present study.

The use of cyprinodontiform fishes, e.g. livebearers (Comfort 1963) and killifish (Markofsky & Perlmutter 1972), has a long tradition in biological research although histological studies have focused mainly on individual organs and systems; exemplified by a detailed study on the intestinal histology and histopathology of parasitic infections in *Gambusia affinis* (Bullock 1967) and a study on the histology of the digestive tract of *Fundulus heteroclitus* (Ciullo 1968). Recent studies on cyprinodontiform histology include descriptions of anatomy and histology of major organ systems in *Aphanius hormuzensis* (Motamedi et al. 2019) and histology of the digestive tract of *Aphanius persicus* (Monsefi et al. 2010). To our knowledge, there have been no studies on the normal histology of *Nothobranchius* species since the pioneering works of Markofsky (1979) and Markofsky & Milstoc (1979). However, a need for this work is pressing as *Nothobranchius* species have emerged as a fish model with increasing importance in toxicology (Philippe et al. 2018), biomedicine (Hu & Brunet 2018), regeneration research (Wang et al. 2020) and evolutionary ecology (Reichard & Polačik 2019).

Nothobranchius species are short-lived teleosts with an annual lifespan and thus represent practical model organisms in a variety of disciplines. Among these fishes, *Nothobranchius furzeri* is the most commonly used. The short lifespan of this species represents an adaption to periodically desiccating savannah pools in Africa (Kenya: NP; Mozambique: NF; Tanzania NA, NE, NG, NR) and is typified by rapid maturation, fast growth, desiccation resistant embryos and short lifespan (Reichard & Polačik 2019). There is a minimal morphological disparity across *Nothobranchius* spp. and they are ecologically similar (Lambert et al. 2019). They are amenable to captive breeding and several breeding protocols are available, making them practical fish models for laboratory research (Polačik et al. 2016, Philippe et al. 2018, Astre et al. 2022).

The aims of our study are to provide an overview of the histology of *Nothobranchius* fishes, to underline some characteristic features of this genus, and identify challenging topics for research. We provide a short condensed introductory text and incorporate most information in figure captions. The pictorial design of our study provides a guideline for comparisons with other fish species and enables interpretation of microscopically detectable changes in various tissues. We anticipate our atlas will serve as a reference for *Nothobranchius* researchers from varied backgrounds. We acknowledge that our study does not cover the histology of all organs and tissues, which is not a realistic task. In addition, some tissues/organ systems are omitted intentionally because they are already subjects of specialised accounts (e.g. nervous system and integument, D'Angelo 2013, Do et al. 2021).

Material and Methods

Nothobranchius material examined in this study originated primarily from the breeding laboratory at the Institute of Vertebrate Biology, Czech Academy of Sciences, Czech Republic and partly was provided by hobbyists interested in the health status of their stocks. A small number of specimens were collected in natural habitats. It is specified in figure captions when wild specimens were investigated, otherwise specimens were from captivity. In total, over three hundred individuals of six species from different age categories were used in this study.

In order to visualize the structure of *Nothobranchius* organs and tissues, we examined and documented traditionally used paraffin sections, as well as semi-thin sections of resin-embedded material, using a light microscope (Olympus BX 60 equipped with digital camera DP 71). Transmission electron microscopy (JEOL 1010, Japan) was used to examine and document selected material at a cellular and subcellular level. The paraffin technique and standard staining methods were applied in accordance with standard manuals and textbooks on histology including the 8th edition of "Bancroft's theory and practice of histological techniques" (Suvarna et al. 2018).

The age of specimens used was categorised as larval (0-5 dph), juvenile (6-30 dph), adult (31-140

dph), and senescent (140+ dph). *Nothobranchius furzeri* at age 140+ dph are considered as senescent for all the populations examined (GRZ, MZM 0410, MZCS 222 in accordance with Cellerino et al. 2016) and this was the only species for which senescent specimens were investigated.

For semi-thin and ultra-thin sectioning the samples were fixed with 2% osmium tetroxide, dehydrated with acetone of increasing concentrations and embedded in Spurr resin. Semi-thin sections were stained with toluidine blue; ultra-thin sections were double stained with uranyl acetate and lead citrate according to the standard procedure described in Dykstra (1993). Light microscopy of semi-thin sections supplemented paraffin histology and was adopted particularly for the early larval stages. Electron micrographs were used to demonstrate unique and undescribed structures in *Nothobranchius* species and to demonstrate changes at the cellular level.

Results and Discussion

Digestive tract

Histological data for the digestive tract of *Nothobranchius* fishes are presented in common with the most comprehensive review of gastrointestinal tract diversity in fishes by Wilson & Castro (2010). For comparative reasons, four segments of gut related to topographical regions of the fish body, i.e. headgut, foregut, midgut and hindgut, are described with the emphasis on the segments in which digestion and absorption take place.

The headgut, composed of the mouth, oral cavity and pharynx, where the capture and initial mechanical processing of food take place, differs substantially from the other subdivisions of the alimentary tube. The mouth with lips is covered by nonkeratinized stratified squamous epithelium (Fig. 1a). There are several rows of jaw teeth and the planes of our histological sections displayed just one conus in the crown of the jaw teeth (Fig. 1a, b) because *Nothobranchius* species have conical and fang-shaped jaw teeth (Costa 2018). This arrangement is in contrast to *Aphanius* spp., for example, which have tricuspid teeth (Monsefi et al. 2010). The oral cavity and the oral valves (sensu Kardong 2012) are lined by a thin layer of stratified epithelium with individual goblet cells (Fig. 1c). The pharynx, the most aboral pre-esophageal part of digestive tract, is lined with a much thicker layer of stratified epithelium that contains numerous sensory cells forming taste buds (Fig. 1d). In the headgut there are also pharyngeal teeth (Fig. 1e, f).

The postpharyngeal part of digestive tract, referred to as the foregut, consists of the oesophagus and stomach in approximately 80% of teleost species (Wilson & Castro 2010). In contrast, Cyprinodontiformes are classified as agastric fishes (Wilson & Castro 2010) and they do not possess submucosal multicellular gastric glands like other agastric species (Chao 1973). Within the Cyprinodontiformes, *A. persicus* has been suggested as an exception (Monsefi et al. 2010), though the evidence is not convincing. Unfortunately, the dilated digestive tube segment described by Monsefi et al. (2010) as containing "short simple branch tubular glands" is not documented in their paper, although they focus on the digestive tract. In another species of this genus (*A. hormuzensis*), the stomach is not mentioned among the briefly characterized digestive tract segments (Motamedi et al. 2019).

Despite careful examination of numerous series of cross and longitudinal sections through the digestive tube of *Nothobranchius*, we found no segment with gastric glands. This finding supports the view that the foregut of *Nothobranchius* spp. consists of the oesophagus only (Fig. 2a). The oesophageal structure is essentially the same as in other teleosts, including those of gastric groups. A thick-walled oesophagus is characterized by longitudinal mucosal folds covered with stratified epithelium with abundant mucus cells forming a continuous luminal layer (Fig. 2b). A subepithelial connective tissue layer is intertwined with striated muscle bundles (Fig. 2c). There is a well-defined transition between the oesophageal and intestinal/midgut epithelia (Fig. 3a) seen as an abrupt disappearance of the mucous cells, absence of striated muscle bundles and presence of massive longitudinal mucosal folds (Fig. 3a, b). In the anterior part, the midgut wall consists of simple mucosal folds with individual goblet cells interspersed among the absorptive cells (Figs. 3b, 5b), subepithelial loose connective tissue with capillary network, and smooth muscle fibres in two layers; the inner one with circular and the outer one with longitudinal orientation (Fig. 3b). We did not find clearly defined subdivisions of the midgut, although the number of goblet cells scattered throughout the cylindrical epithelium differed substantially in irregularly branching intestinal folds (compare Figs. 3, 4). We believe

a subdivision of the midgut might become apparent when location of the digestive gland duct orifices is known. Recognition of individual midgut subregions might also be facilitated by a detailed study of the distribution of columnar absorptive cells with distinctive apical brush border, as well as a study of the density and height of microvilli (Fig. 5c, d).

The transition from midgut to hindgut (rectum and anus) is seen as a noticeable narrowing of the midgut diameter (Fig. 6a). The circular muscle layer forms a structure resembling an ileorectal valve described in some teleosts (Wilson & Castro 2010). This feature is clearly visible in longitudinal sections (Fig. 6a, b). However, the continuous circular arrangement of muscle and connective tissue fibres seen in the overview of the cross section through the larval digestive tube (Fig. 7) gives the impression of a sphincter-like structure. The presence of this structure in adult fishes is accompanied with pronounced differences in morphology and staining properties of enterocytes. H&E staining illustrates that rectal columnar cells contain slightly stained prominent apical vacuoles with numerous granules of varying size (Fig. 8b). The same applies to PAS staining. Posteriorly in the rectum, the number of mucus cells decreases gradually and then increases again around the anus. The comparison with the results of a study by Bullock (1967) on *G. affinis* suggests that the rectum may also be involved in nutrient absorption in heavily fed fish.

The posterior part of rectum is characterized by a thick muscle tissue layer of the sphincter and pronounced mucosal folds (Fig. 8c). These structures get thinner towards the terminal part of the tube and disappear where the rectum approaches the anus. The anus is surrounded by an anal papilla composed of extensive fibrous connective tissue covered with stratified epithelium (Fig. 9a). Low magnification images of the anal region clearly show that the anus is, in a caudal direction, followed by the genital orifice, which is followed by the most caudally situated urinary tract orifice (Figs. 8c, 9b). This finding is in conflict with the description of *N. furzeri* body cavity dissection by Astre et al. (2022) who mentioned (p. 269), but did not document, the presence of a cloaca; generally defined as a common passageway for faeces, urine and reproduction organ products or as a common cavity for the excretion of both the excretory and genital products in vertebrates (Kardong 2012).

Transverse and longitudinal sections of larval stages examined 24 hours post hatching (hph) were characterized by the presence of unresorbed yolk in the body cavity and an enormous distention of the midgut caused by consumption of a large amount of *Artemia* nauplii. This condition resulted in the almost complete disappearance of the mucosal folds (Fig. 10a). The brush border of enterocytes was well developed and absorption activity of enterocytes was also evident (Fig. 10b, c).

Digestive glands

The digestive glands, i.e. liver and pancreas, are critical for agastric digestion in killifish because they lack gastric gland secretion. The liver parenchyma of *Nothobranchius* fishes is composed primarily of hepatocytes, the cells are polyhedral in shape and variable in cytoplasmic content due to their ability to deposit either lipids or glycogen (Figs. 11a-c, 12a, c). There is little connective tissue in this organ. Hepatocytes are arranged in two cell cords but acinar/lobular structures, often well defined in vertebrates (Evensen 2006), are absent or not easily discernible. Bile canaliculi are well defined among adjacent hepatocytes, but are incidentally also observed as intracellular structures (Fig. 12b, c). Ultrastructural investigation of the cell compartment condition of hepatocytes is an important supplement to findings obtained from light microscopy of paraffin sections (Figs. 12, 13), and our unpublished observations show that they may be valuable in studies on the effect of different diets. Bile channel hierarchy is difficult to determine in histological sections cut in extrahepatic planes. Sectioning planes are crucial for discerning the organisation of the biliary tree (Fig. 14a-c) because the liver is a slightly asymmetrical organ. Also, the topography of the intestinal outlet of the bile duct should be studied in relation to the histological characteristics of the preceding and following segments. This issue appears especially important in agastric fishes, including *Nothobranchius*.

The pancreas of *Nothobranchius* spp., comparable in structure with many other teleosts, is diffused throughout the body cavity and surrounds various organs, especially the digestive tube. This organ is present in two morphologically and functionally distinct forms, exocrine and endocrine (Fig. 15). Of these, voluminous exocrine glandular tissue predominates in extrahepatic sites but small aggregates (acini) of exocrine tissue are also located in the liver parenchyma (Fig. 15a). Tiny aggregates were found also incidentally in the

intestinal wall (Fig. 14d). Small, compact endocrine units encapsulated in connective tissue, i.e. islets of Langerhans, were found exclusively within extrahepatic exocrine glandular tissue (Fig. 15c). At the light microscopic level, the types and arrangement of exo- and endocrine cells do not differ from those known in other teleosts. We were unable to locate ducts expected to transport secretion products of pancreatic acini despite the examination of abundant embedded material. It was also relatively difficult to distinguish intralobular from main excretory ducts. A confusing situation also arises from entanglement of bile ducts in the pancreatic tissue.

Kidney

The kidney is a bilaterally symmetrical organ composed of anterior bean-shaped regions localized in a retroperitoneal "cephalic" position (Figs. 16a, 19a) and two long collecting/urinary ducts (Fig. 16b). These extend under the vertebral column along the entire body cavity, unify at the level of the anal fin and open to the outside posterior to the anus and genital orifice (Fig. 9b). The kidney contains elements of an excretory system (Figs. 16, 17, 18), hemopoietic and mononuclear phagocytic systems (Figs. 19, 20) and also endocrine tissue (Figs. 38c, 39).

The trunk (posterior/excretory) kidney consists of glomerular nephrons, i.e. renal corpuscles that contain capillary networks (glomeruli) interconnected with a system of tubules, ducts and a supporting matrix of interstitial tissue with hemopoietic cells (Fig. 16c). As in other teleosts, glomeruli (Figs. 16c, 17a) are covered with an outer (parietal) and inner (visceral) layer of Bowman's capsules, in which it is possible to recognize cellular structures described in mammals, i.e. podocytes (with characteristic pedicels) separated by slits (Fig. 18c). These structures, together with endothelial fenestrations, facilitate filtration of liquid from plasma into the urinary space of the renal corpuscle. Renal corpuscles continue on their tubular pole as the neck segment (Fig. 17b), proximal, intermediate and distal segments of the excretory tubules, which are not yet histologically clearly defined (Fig. 17c), and a collecting duct system. The urinary duct, extending from the anterior to posterior abdomen, is thin-walled, with columnar epithelium surrounded by a thin layer of connective tissue and barely detectable circular fibres of smooth muscle tissue. It is associated with a small (in parasagittal sections almost invisible) volume of kidney tissue covered with tunica adventitia (Fig. 16b). In the urinary tract we found no sac-like structure (urinary bladder). Ventrally, under the posterior segment of the urinary duct, always in the same location, Stannius bodies (corpuscle of Stannius) were found whose function has not yet been fully characterised (Fig. 38a, b).

The most anterior and proportionally smallest part of kidney, the head kidney (Fig. 19a), does not differ from the head kidney of most other teleosts. In adult *Nothobranchius* individuals, in contrast to early post-hatching stages, this part of the kidney is not sharply delimited from the posterior part with a dominant proportion of excretory tissue components. As visualised from the topography of these two kidney segments at the larval stage (Fig. 19a, b), sampling of the tiny "true" head kidney is difficult. Head kidney tissue is composed mainly of stem/blast mononuclear cells (progenitors of blood cells and precursors of mononuclear macrophages) the ultrastructure of which differs in accordance with differentiation of their cellular compartments (Fig. 20a, b).

Interrenal tissue, considered to be an adrenal gland homologue in bony fish (Civinni et al. 2001, Gallo & Civinini 2003), was found in close proximity to the posterior cardinal vein passing through hemopoietic tissue of the head kidney (Figs. 38c, 39a).

The terms "head" and "trunk" kidney were introduced into the literature years ago, being synonymous for the anterior hematopoietic and the posterior excretory part of this organ, respectively. In fish with a more-or-less clear anatomical division of these kidney parts, this terminology also serves as an approximate indication of their location. *Nothobranchius* do not have these two parts clearly separated but we decided to follow traditional usage in ichthyology, fish physiology, histology and histopathology books and papers (Anderson & Mitchum 1974, Roberts 1978, Ferguson 2006, Morrison et al. 2006, Bruno et al. 2013, Bjorgen & Koppang 2021) in order to avoid confusion (such as in Astre et al. 2022).

Spleen

As in most teleosts, the spleen of *Nothobranchius* fishes is an accessory hemopoietic organ with haemoblasts less abundant than in the head and trunk kidney. Its histological structure differs essentially from that of the mammalian spleen in two respects. Red and white pulp are diffuse, not

sharply delimited (Fig. 21). The connective tissue framework (trabecular system) is not prominent. The red pulp, which usually comprises the majority of the splenic parenchyma, is composed of sinusoids filled with erythroid cells, erythrocytes, and thrombocytes (Fig. 22a) coupled with an interconnecting system of splenic cords consisting of fibroblast-like cells. The white pulp, which is formed mainly by haemoblasts and lymphoid cells (Fig. 22b, c), contains ellipsoids formed as periarterial sheets with mononuclear cells of the phagocytic system, fibrocytes and reticular fibres. Cells of the mononuclear phagocytic system (MPS) are able to trap particulate material such as effete blood cells including aged erythrocytes (Fig. 22d). We did not find clearly delimited germinal centres.

Fish do not possess bone marrow; however, the hemopoietic environment in teleosts is well developed in the head kidney, interstitial tissue of trunk kidney, and spleen (Ellis 1982). Several authors (Davidson & Zon 2004, Havixbeck & Barreda 2015, Avagyan & Zon 2016) introduced the term "kidney marrow" in attempts to compare haematopoiesis in fish and mammals. In a way, this is understandable since it was shown that the developmental hierarchy of myeloid cell precursors in zebrafish is similar to that in humans and the morphological and molecular genetic evidence supports the zebrafish as an informative model for the study of normal and aberrant human myelopoiesis (Bennett et al. 2001, Avagyan & Zon 2016). Recently, Bjorgen & Koppang (2021) have been critical of the simplifying concepts presented by researchers dealing with the zebrafish model. Indeed, the birthplace of the hemopoietic stem cells persisting throughout the lives of mammals and fish differ. In mammals it is bone marrow, whereas in fish it is the hemopoietic tissue of the kidney.

Mononuclear phagocyte system and macrophage aggregates

Histopathological misinterpretations in the literature and results of our own study (Dyková et al. 2021b) prompted us to include a short section on the *Nothobranchius* mononuclear phagocyte system, especially the tissue macrophages. The mononuclear phagocyte system, previously referred to as the reticuloendothelial system (RES), was renamed the MPS by van Furth et al. (1972) in order to distinguish macrophages from polymorphonuclear leukocytes or neutrophils and to show that all macrophages originate via terminal differentiation from blood monocytes. This widely accepted concept has been slightly modified relatively recently in the light of a detailed study of MPS in zebrafish (Wittamer et al. 2011). In *Nothobranchius,* the MPS also comprises peripheral blood monocytes, tissue macrophages and dendritic cells as well as their lineage-committed progenitors. Mononuclear cell populations of hematopoietic tissues (consisting of stem and progenitor cells) do not differ substantially from blood monocytes based on their morphology. The capacity for particle uptake, however, makes monocytes/macrophages important members of the mononuclear phagocyte system (MPS) and thus contributors to fish immunity.

Mononuclear cells of the MPS were observed to form aggregates (MAs) of variable size, shape and organ distribution (Figs. 23, 24), usually in close vicinity to blood vessels. Mononuclear aggregates may have been misdiagnosed as tumours in some studies of *Nothobranchius* tumorigenesis published in the last two decades. Thus, immune reactions in tissues deserves special attention. The occurrence of MAs was associated in *Nothobranchius* fishes with endogenous stimuli such as cellular degradation products or exogeneous material including prokaryotes and eukaryotes (Figs. 24, 25). Effete red and white blood cells and biological agents were commonly observed within macrophages. An enormous proliferative capacity of monocytes/macrophages was observed in response to *Glugea* and *Mycobacterium* infections. In the latter infection, we also encountered an unconventional coiling type of phagocytosis (Fig. 25b). Stellate or elongate cells with filaments emanating from the cell body and numerous cytoplasmic granules were observed mainly in the spleen (Fig. 26a, d). Their morphology matched that of dendritic cells (DCs) described in detail by Puhr et al. (2015) as cells forming the link between the innate and adaptive immune system in mammals. Lugo-Villarino et al. (2010) described DCs as antigen presenting cells (APCs) in zebrafish. Their presence and function in other non-mammalian vertebrates is still largely unknown.

The tissue resident macrophage centres reported in most teleosts as melanomacrophage centres (MMC), due to their pigmented content (Wolke 1992), were rarely observed in short-lived *N. furzeri* and never with a high pigment content (Fig. 23a-c). In contrast, we detected well-pigmented macrophages scattered in the subepithelial connective tissue of the intestine and concentrated

in the liver of long-lived laboratory reared *N. guentheri* (Fig. 23d).

Swim bladder

Observed histopathological changes in the swim bladder of *Nothobranchius* fishes (Dyková et al. 2020, 2021a) prompted us to revise the data on this subject, learn more about the structure of this organ, and determine whether *Nothobranchius* spp. belong to physostomous, physoclist or euphysoclist fishes (Lumsden 2006). We found the histological study of this problem to be difficult because of the small size of this thin-walled organ that collapses easily, and because of difficulties in standardization of the plane of sectioning that is crucial for comparison and correct interpretation of findings. In view of our histological results on the senescent (Dyková et al. 2020) and early life stages of the killifish swim bladder (Dyková et al. 2021a), we examined extensive material (more than a thousand semi-thin parasagittal sections) from individuals fixed ten days post hatching. We did not find any interconnection between the digestive tract and the swim bladder, and subsequently assessed additional material from younger fish (8 and 24 hours post hatching; hph). Again, no connection of the digestive tube with the swim bladder was found. In conclusion, we can confidently assign *Nothobranchius* spp. to physoclist fishes with the swim bladder as a closed gas cavity organ.

Swim bladders examined in three *Nothobranchius* species comprised a single cavity organ of ovoid shape with a thick wall anteriorly (Figs. 27a, b, 28c) where it is interconnected with an extensive capillary system and a gas gland. The latter is a several layer complex of epithelial cells with secretory/resorbing cytoplasmic characteristics that differ from those of the internal epithelium (Fig. 27c). Posteriorly, the thin wall of the swim bladder consists of membranous connective tissue internally lined by simple epithelium (Figs. 27d, 28c).

Although a great majority of teleosts are physoclists (Pelster 2011), their swim bladders differ substantially in general morphology and fine structure. The delicate structure of *Nothobranchius* swim bladders are not easy to compare with results for the robust type of swim bladder of the European eel, which has been studied in detail as a model for the analysis of swim bladder function (Pelster 2015). In terms of the fine structure, the *Nothobranchius* swim bladder is challenging in terms of ascertaining whether the two physiological phenomena associated with swim bladder function (gas secretion and gas resorption) are manifested by corresponding types of epithelial cells.

Other organs and tissues

For completeness, some other organ structures, such striated skeletal muscle (Figs. 29, 30), heart (Figs. 31, 32), ovaries (Fig. 33), testes (Fig. 34), gills (Fig. 35), pseudobranchia (Fig. 36), thymus (Fig. 37) and tissues with endocrine activity (Figs. 38, 39, 40) are presented with self-explanatory figure captions.

Summary

The description of normal structure is of essential importance for understanding the functions and abnormalities of organs and tissues in any organism. Here, we present the normal structure in various organs and tissues of *Nothobranchius* spp., an emerging model organism in multiple fields of biological research (Hu & Brunet 2018, Philippe et al. 2018, Reichard & Polačik 2019). We entirely concur with Wilson & Castro (2010) for whom morphology is "far from being a dying line of investigation". We believe that histological and ultrastructural research will continue the exploration of the organ and tissue characteristics of annual killifishes, which is fundamental to the proper utilisation of these models in biological research.

Acknowledgements

This work was supported by a grant from the Czech Science Foundation 19-20873S. We thank Gabriela Vágnerová for assistance during preparation of histological samples; Matej Polačik and Milan Vrtílek for comments on an early version of the manuscript. All procedures involving laboratory animals were conducted according to all institutional and national legal regulations of the Czech Republic. Sample collection of wild fish used in the present study complied with legal regulations of Mozambique (collection licence issued by Mozambican Ministry of Sea, Inland Waters and Fisheries: ADNAP-170/7.10/16). Author contributions (in accordance with the CRediT): Conceptualization: I. Dyková, J. Žák; Methodology: I. Dyková; Validation: I. Dyková, J. Žák; Investigation: I. Dyková, J. Žák, R. Blažek, K. Součková; Resources: I. Dyková, R. Blažek, M. Reichard; Data curation: I. Dyková, J. Žák; Writing – original draft: I. Dyková, J. Žák; Writing – Review & Editing: R. Blažek, M. Reichard, K. Součková, O. Slabý; Visualization: I. Dyková, J. Žák; Supervision: I. Dyková; Funding acquisition: R. Blažek, K. Součková, O. Slabý.

Literature

Anderson B.G. & Mitchum D.L. 1974: Atlas of trout histology. *Wyoming Game & Fish Department, USA.*

Astre G., Moses E. & Harel I. 2022: The African turquoise killifish (*Nothobranchius furzeri*): biology and research applications. In: D'Angelo L. & de Girolamo P. (eds.), Laboratory fish in biomedical research. Biology, husbandry and research applications for zebrafish, medaka, killifish, platyfish, cavefish, stickleback, goldfish and *Danionella translucida*. *Elsevier Science: 245–287.*

Avagyan S. & Zon L.I. 2016: Fish to learn: insights into blood development and blood disorders from zebrafish hematopoiesis. *Hum. Gene Ther. 27: 287–294.*

Bennett C.M., Kanki J.P., Rhodes J. et al. 2001: Myelopoiesis in the zebrafish, *Danio rerio*. *Blood 98: 643–651.*

Bjorgen H. & Koppang E.O. 2021: Anatomy of teleost fish immune structures and organs. *Immunogenetics 73: 53–63.*

Bruno D.W., Noguera P.A. & Poppe T.T. 2013: A colour atlas of Salmonid diseases. *Springer Science + Bussines Media.*

Bullock W.L. 1967: The intestinal histology of the mosquito fish, *Gambusia affinis* (Baird and Girard). *Acta Zool. 48: 1–17.*

Cellerino A., Valenzano D.R. & Reichard M. 2016: From the bush to the bench: the annual *Nothobranchius* fishes as a new model system in biology. *Biol. Rev. 91: 511–533.*

Chao L.N. 1973: Digestive system and feeding habits of the cunner, *Tautogolabrus adspersus*, a stomachless fish. *Fish. Bull. 71: 565–586.*

Ciullo R.H. 1968: The histology of the digestive tube of the Cyprinodontiform fish, *Fundulus heteroclitus* (Linnaeus). *PhD thesis, University of New Hampshire, USA.*

Civinni A., Padula D. & Gallo V.P. 2001: Ultrastructural and histochemical study on the interrenal cells of the male stickleback (*Gasterosteus aculeatus*, Teleostea), in relation to the reproductive annual cycle. *J. Anat. 199: 303–316.*

Comfort A. 1963: Effect of delayed and resumed growth on the longevity of a fish (*Lebistes reticulatus*, Peters) in captivity. *Gerontologia 8: 150–155.*

Costa W.J.E.M. 2018: Comparative morphology, phylogeny and classification of African seasonal killifishes of the tribe Nothobranchiini (Cyprinodontiformes: Aplocheilidae). *Zool. J. Linn. Soc. 184: 115–135.*

D'Angelo L. 2013: Brain atlas of an emerging teleostean model: *Nothobranchius furzeri*. *Anat. Rec. 296: 681–691.*

Davidson A.J. & Zon L.I. 2004: The "definitive" (and 'primitive') guide to zebrafish hematopoiesis. *Oncogene 23: 7233–7246.*

Do E., Lee S. & Kim Y. 2021: Anatomical identification of the neuroendocrine system in the *Nothobranchius furzeri* brain. *J. Vertebr. Biol. 70: 21018. https://doi.org/10.25225/jvb.21018*

Dyková I., Blažek R., Součková K. et al. 2020: Spontaneous adenocarcinoma of the gas gland in *Nothobranchius* fishes. *Dis. Aquat. Org. 137: 205–210.*

Dyková I., Žák J., Reichard M. et al. 2021a: Swim bladder as a primary site of mycobacterial infection in *Nothobranchius* "belly sliders". *Dis. Aquat. Org. 145: 111–117.*

Dyková I., Žák J., Reichard M. et al. 2021b: Histopathology of laboratory reared *Nothobranchius* fishes: mycobacterial infections versus neoplastic lesions. *J. Fish Dis. 44: 1179–1190.*

Dykstra M.J. 1993: A manual of applied techniques for biological electron microscopy. *Plenum Press, New York, USA.*

Ellis A.E. 1982: Differences between the immune mechanisms of fish and higher vertebrates. In: Roberts R.J. (ed.), Microbial diseases of fish. *Academic Press, London: 1–29.*

Evensen O. 2006: Liver. In: Ferguson H. (ed.), Systemic pathology of fish: a text and atlas of normal tissues in Teleosts and their responses in disease. *Scotian Press, London, UK: 201–216.*

Ferguson H.W. 2006: Systemic pathology of fish: a text and atlas of normal tissues in Teleosts and their responses in disease. *Scotian Press, London, UK.*

Gallo V.P. & Civinini A. 2003: Survey of the adrenal homolog in teleosts. *Int. Rev. Cytol. 230: 89–187.*

Havixbeck J.J. & Barreda D.R. 2015: Neutrophil development, migration, and function in teleost fish. *Biology 4: 715–734.*

Hu C.K. & Brunet A. 2018: The African turquoise killifish: a research organism to study vertebrate aging and diapause. *Aging Cell. 17: e12757.*

Kardong K.V. 2012: Vertebrates: comparative anatomy, function, evolution. *McGraw-Hill Education, New York, USA.*

Lambert J.W., Reichard M. & Pincheira-Donoso D. 2019: Live fast, diversify non-adaptively:

evolutionary diversification of exceptionally short-lived annual killifishes. *BMC Evol. Biol. 19: 10.*

Lieschke G.J. & Currie P.D. 2007: Animal models of human disease: zebrafish swim into view. *Nat. Rev. Genet. 8: 353–367.*

Lugo-Villarino G., Balla K.M., Stachura D.L. et al. 2010: Identification of dendritic antigen-presenting cells in the zebrafish. *Proc. Natl. Acad. Sci. U. S. A. 107: 15850–15855.*

Lumsden J.S. 2006: Gastrointestinal tract, swimbladder, pancreas and peritoneum. In: Ferguson H.W. (ed.), Systemic pathology of fish: a text and atlas of normal tissues in teleosts and their responses in disease. *Scotian Press, London, UK: 169–199.*

Markofsky J. 1979: Aging changes in the liver of the male annual cyprinodont fish, *Nothobranchius guentheri*. *Exp. Gerontol. 14: 11–20.*

Markofsky J. & Milstoc M. 1979: Histopathological observations of the kidney during aging of the male annual fish *Nothobranchius guentheri*. *Exp. Gerontol. 14: 149–155.*

Markofsky J. & Perlmutter A. 1972: Age at sexual maturity and its relationship to longevity in the male annual Cyprinodont fish, *Nothobranchius guentheri*. *Exp. Gerontol. 7: 131–135.*

Menke A.L., Spitsbergen J.M., Wolterbeek A.P.M. & Woutersen R.A. 2011: Normal anatomy and histology of the adult zebrafish. *Toxicol. Pathol. 39: 759–775.*

Monsefi M., Gholami Z. & Esmaeili H.R. 2010: Histological and morphological studies of digestive tube and liver of the Persian tooth-carp, *Aphanius persicus* (Actinopterygii: Cyprinodontidae). *IUFS J. Biol. 69: 57–64.*

Morrison C.M., Fitzsimmons K.M. & Wright J.R. 2006: Atlas of tilapia histology. *World Aquaculture Society, USA.*

Motamedi M., Shamsaldini F., Teimori A. & Askari M. 2019: Histomicroscopy and normal anatomy of the adult killifish *Aphanius hormuzensis* (Teleostei; Aphaniidae) from the Persian Gulf coastal environment. *Microsc. Res. Tech. 82: 466–480.*

Pelster B. 2011: Swimbladder function and buoyancy control in Fishes. In: Farell A.P. (ed.), Encyclopedia of fish physiology. *Elsevier, London, UK: 526–534.*

Pelster B. 2015: Swimbladder function and the spawning migration of the European eel *Anguilla anguilla*. *Front. Physiol. 5: 1–10.*

Philippe C., Gregoir A.F., Thoré E.S.J. et al. 2018: Protocol for acute and chronic ecotoxicity testing of the turquoise killifish *Nothobranchius furzeri*. *J. Vis. Exp. 134: e57308.*

Polačik M., Blažek R. & Reichard M. 2016: Laboratory breeding of the short-lived annual killifish *Nothobranchius furzeri*. *Nat. Protoc. 11: 1396–1413.*

Puhr S., Lee J., Zvezdova E. et al. 2015: Dendritic cell development-history, advances, and open questions. *Semin. Immunol. 27: 388–396.*

Reichard M. & Polačik M. 2019: *Nothobranchius furzeri*, an 'instant' fish from an ephemeral habitat. *eLife 8: e41548.*

Roberts R.J. 1978: Fish pathology. *University Press, London, UK.*

Suvarna S.K., Layton C. & Bancroft J.D. 2018: Bancroft's theory and practice of histological techniques. *Elsevier.*

van Furth R., Cohn Z.A., Hirsch J.G. et al. 1972: The mononuclear phagocyte system: a new classification of macrophages, monocytes, and their precursor cells. *Bull. W. H. O. 46: 845–852.*

Wang W., Hu C.K., Zeng A. et al. 2020: Changes in regeneration-responsive enhancers shape regenerative capacities in vertebrates. *Science 369: eaaz3090.*

Wilson J.M. & Castro L.F.C. 2010: Morphological diversity of the gastrointestinal tract in fishes. In: Grosell M., Farrell A.P. & Brauner C.J. (eds.), The multifunctional gut of fish. *Fish Physiol. 30: 1–55.*

Wittamer V., Bertrand J.Y., Gutschow P.W. & Traver D. 2011: Characterization of the mononuclear phagocyte system in zebrafish. *Blood 117: 7126–7135.*

Wolke R.E. 1992: Piscine macrophage aggregates: a review. *Annu. Rev. Fish Dis. 2: 91–108.*

List of abbreviations

APC – antigen presenting cells
DC – dendritic cell
dph – days post hatching
hph – hours post hatching
H&E – haematoxylin and eosin
MA – mononuclear cell aggregates
MMC – melanomacrophage centre
PAS – periodic acid Schiff
MPS – mononuclear phagocyte system
NA – *Nothobranchius annectens*
NE – *Nothobranchius eggersi*
NF – *Nothobranchius furzeri*
NG – *Nothobranchius guentheri*
NP – *Nothobranchius patrizii*
NR – *Nothobranchius rubripinnis*
RER – rough endoplasmic reticulum
RES – reticuloendothelial system
SER – smooth endoplasmic reticulum

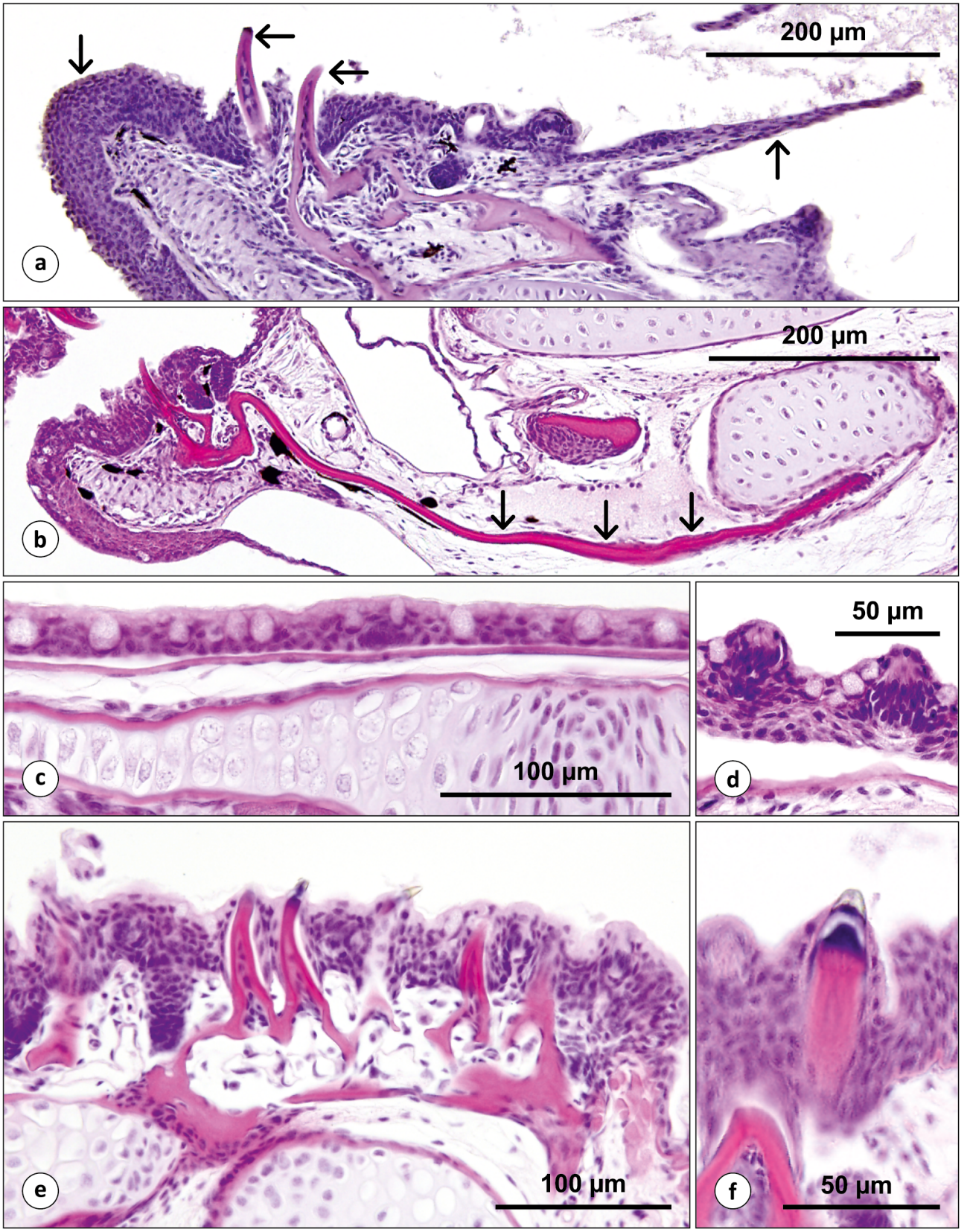

Fig. 1. Headgut. Parasagittal section through the head shows oral cavity details: (a) Lips covered with nonkeratinized stratified squamous epithelium (↓), two conical jaw teeth (←) and breathing valve (↑). (b) Jaw tooth with long root (↓) arising in cartilage of lower jaw. (c) Thin stratified oral cavity epithelium with goblet cells. (d) Taste buds in oral cavity epithelium. (e) Pharyngeal teeth. (f) Detail of pharyngeal tooth. Adult NF (a, d), adult NR (b, c, e, f).

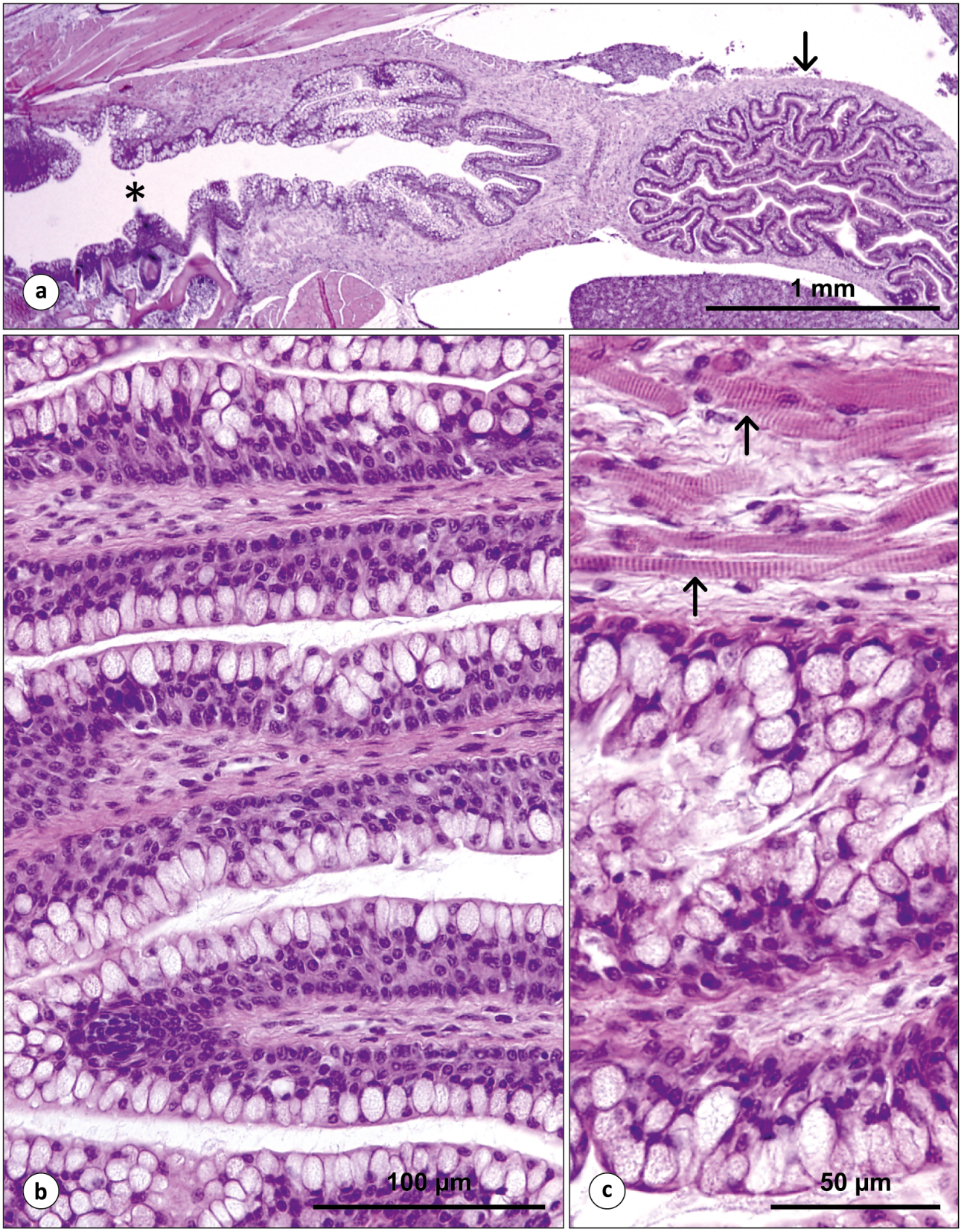

Fig. 2. Foregut. (a) Longitudinal section of gut (presented at low magnification) shows transition of pharynx into oesophagus (*) and a part of the intestine (↓). (b) Large saccular mucus cells (different from goblet cells) dominate in oesophageal multi-layered epithelium which forms a continuous layer lining the luminal side of mucosal folds. **(c)** Wall of oesophagus contains bundles of striated muscle fibres (↑) in subepithelial connective tissue and lamina muscularis. Adult NF.

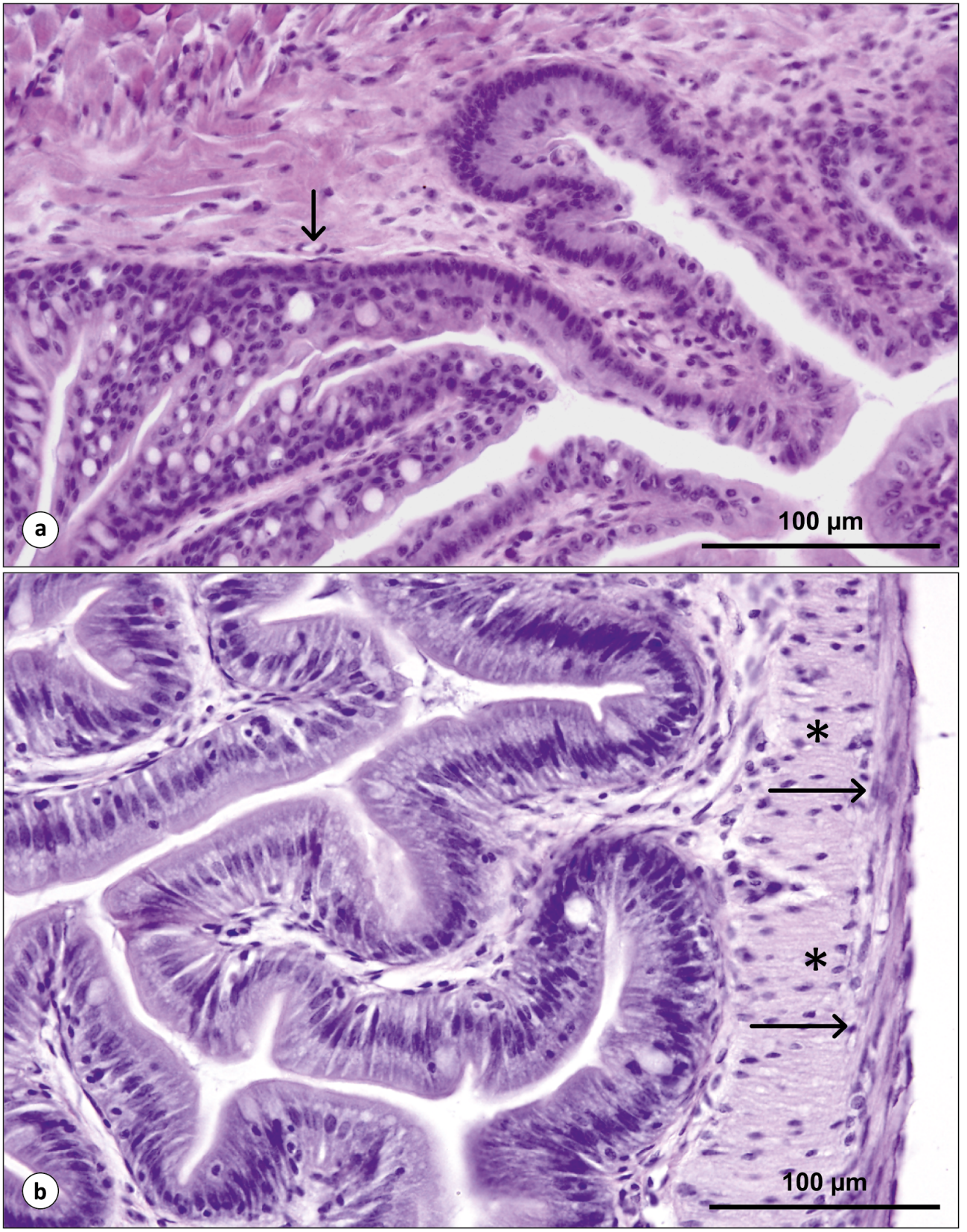

Fig. 3. Midgut I. Part of intestine where chemical digestion and absorption occur in (agastric) *Nothobranchius* fishes. (a) Transition of foregut (represented in these fishes by oesophagus) into midgut (intestine) seen in longitudinal section (↓). (b) Transverse section of midgut. Mucosal folds are covered with simple columnar epithelium; the outer layer of the digestive tube contains muscle fibres oriented in an inner circular (*) and an outer (longitudinal) layer (→). Adult NE (a), adult NF (b).

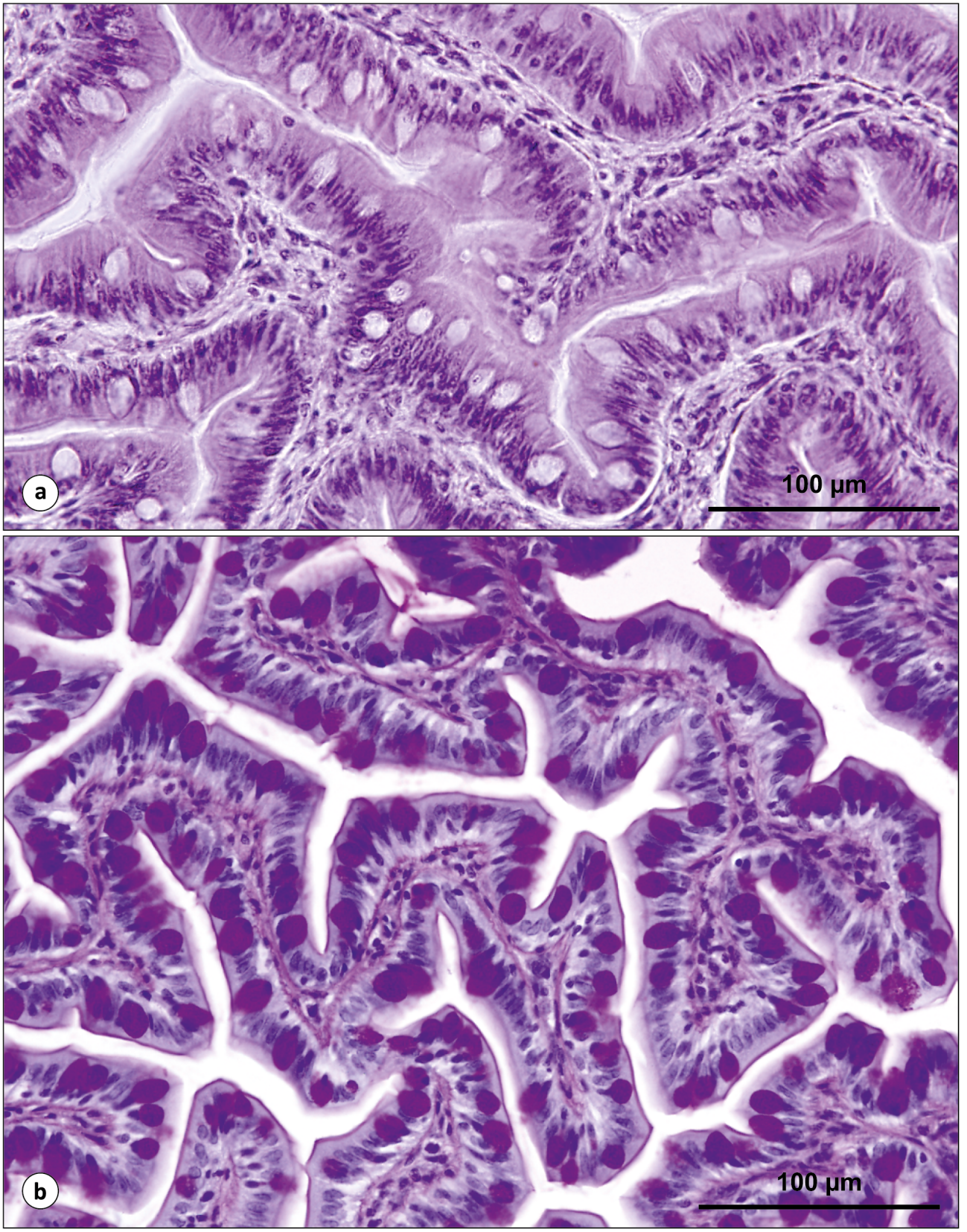

Fig. 4. Midgut II. Segment of midgut with numerous goblet cells. Branching mucosal folds are presented in random section plane. (a) Goblet cells stained with H&E shown as empty spaces in epithelial lining of mucosal folds. (b) Periodic acid Schiff reaction (PAS), specific red staining for mucopolysaccharides, visualizes mucus in goblet cells and in a thin layer on the surface of mucosa. Adult NF.

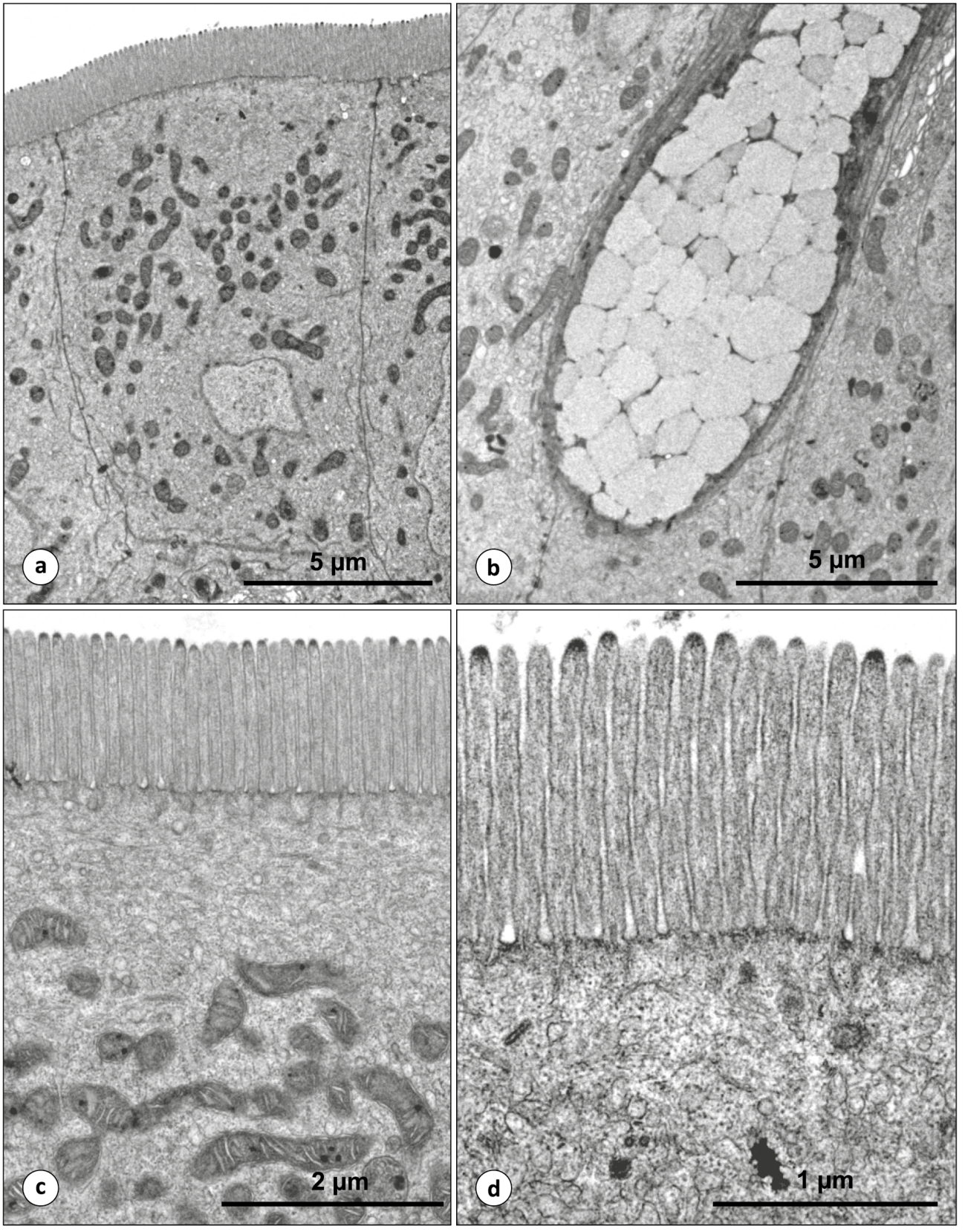

Fig. 5. Ultrastructure of midgut epithelium. (a) Enterocyte, the cell of simple columnar epithelium lining intestinal lumen, with distinctive striated/brush border, numerous mitochondria and nucleus seen in relatively small profile. (b) Goblet cell with multiple mucin granules intermingled among enterocytes. (c, d) Densely packed microvilli, arranged in parallel, extend from free apical parts of enterocytes and form brush border greatly enhancing surface area for absorption. Adult NF.

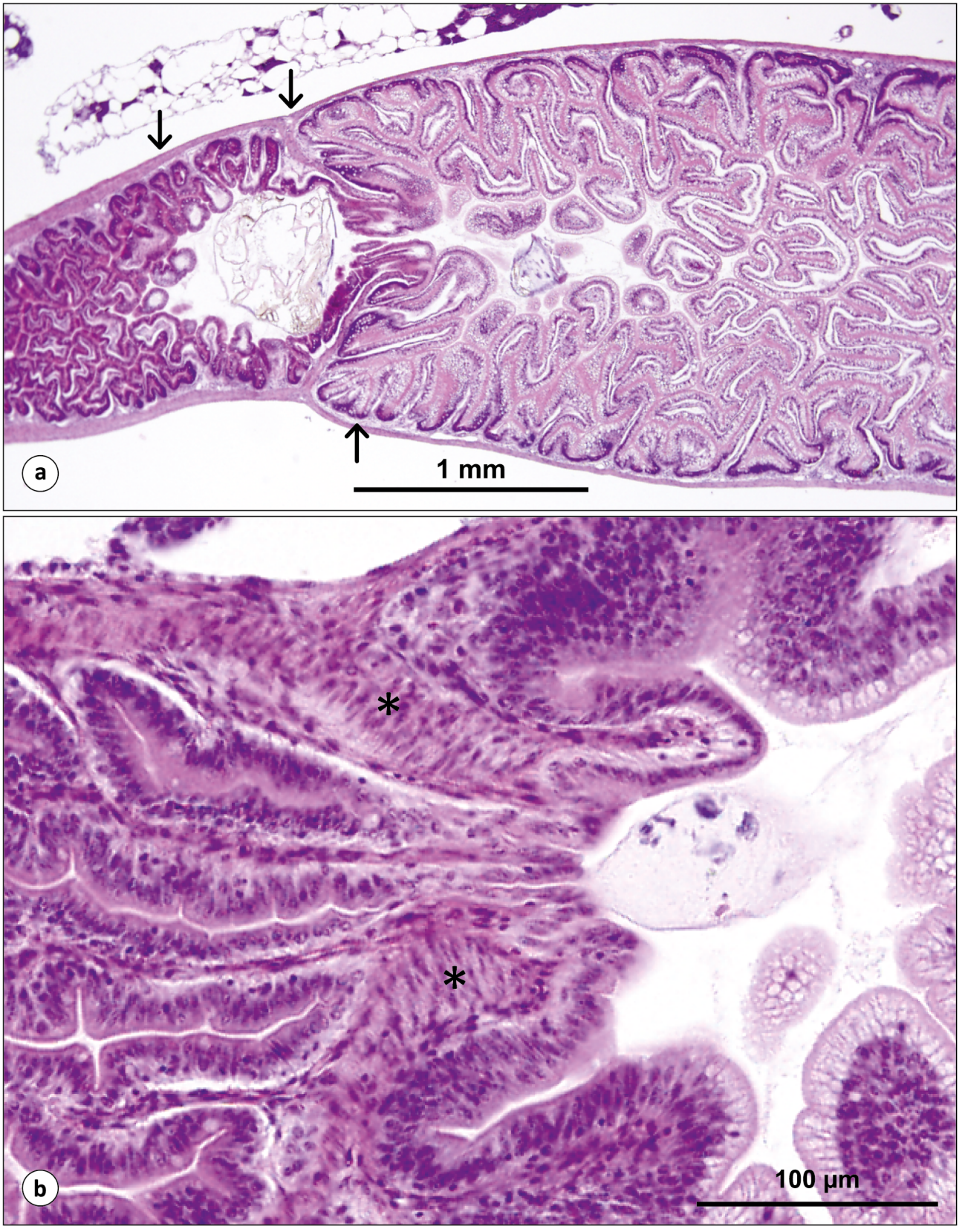

Fig. 6. Hindgut. (a) Longitudinal section of digestive tube showing transition of midgut (↓) into hindgut (↑), giving the impression of intussusception of intestine into rectum. (b) Higher magnification of the transition. In the literature this transition in teleosts has been termed the gut valve, but it is shown here that the transition actually consists of a narrowing of the intestinal lumen due to conspicuously thick lamina muscularis (*). Adult NF (a), adult NR (b).

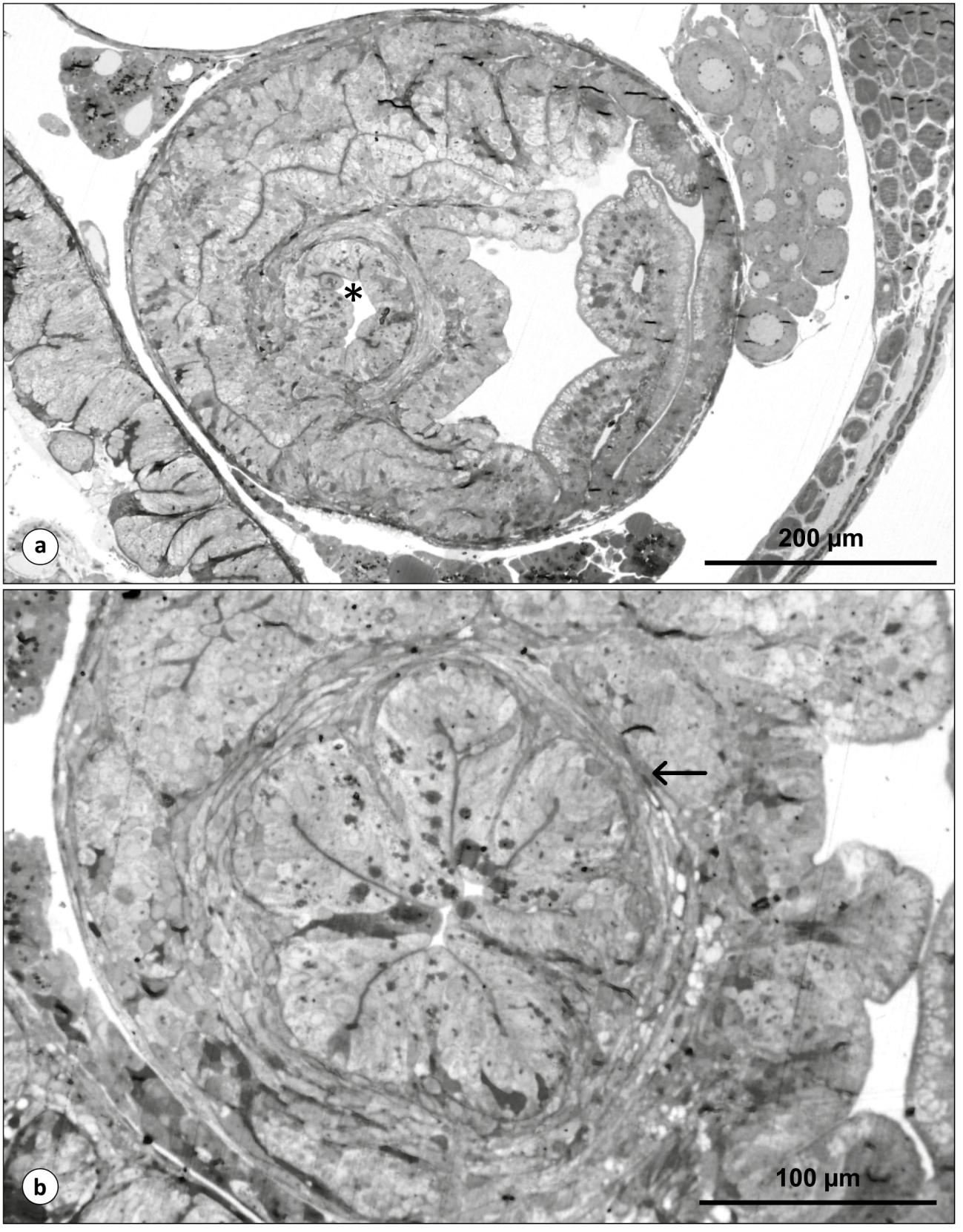

Fig. 7. Larval midgut and hindgut. (a) Transition of larval midgut into hindgut seen in transverse semi-thin section. Invagination of midgut into rectum manifests itself by two lumina. The smaller lumen (*) associated with the midgut, the larger to the rectum. (b) Continuous layer of muscle and connective tissue fibres (←) of intestine invaginated into rectum at this part of the intestinal wall can be considered a sphincter-like structure. NF.

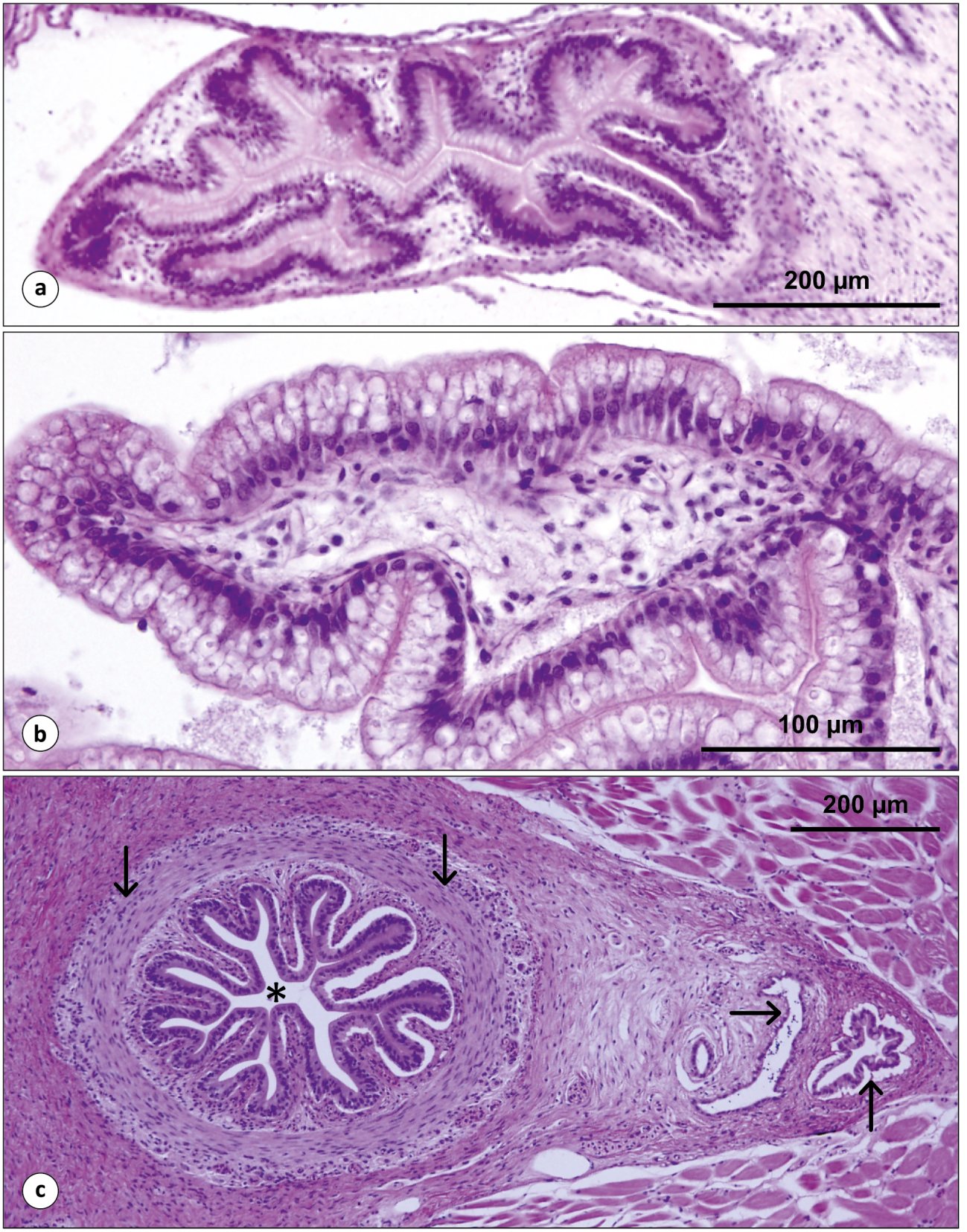

Fig. 8. Rectum. (a) Posterior segment of rectum. (b) Mucosal fold of rectum lined with columnar epithelium. In supra-nuclear position the epithelial cells have voluminous vacuoles which contain mucus-like substances and most of them also contain granules. (c) Tangential longitudinal section through ventral part of belly. Left, anus (*) with a prominent circular muscle layer (↓) (sphincter). Male genital duct (→) and urinary duct (↑) are located more caudally. Adult NR (a), adult NF (b, c).

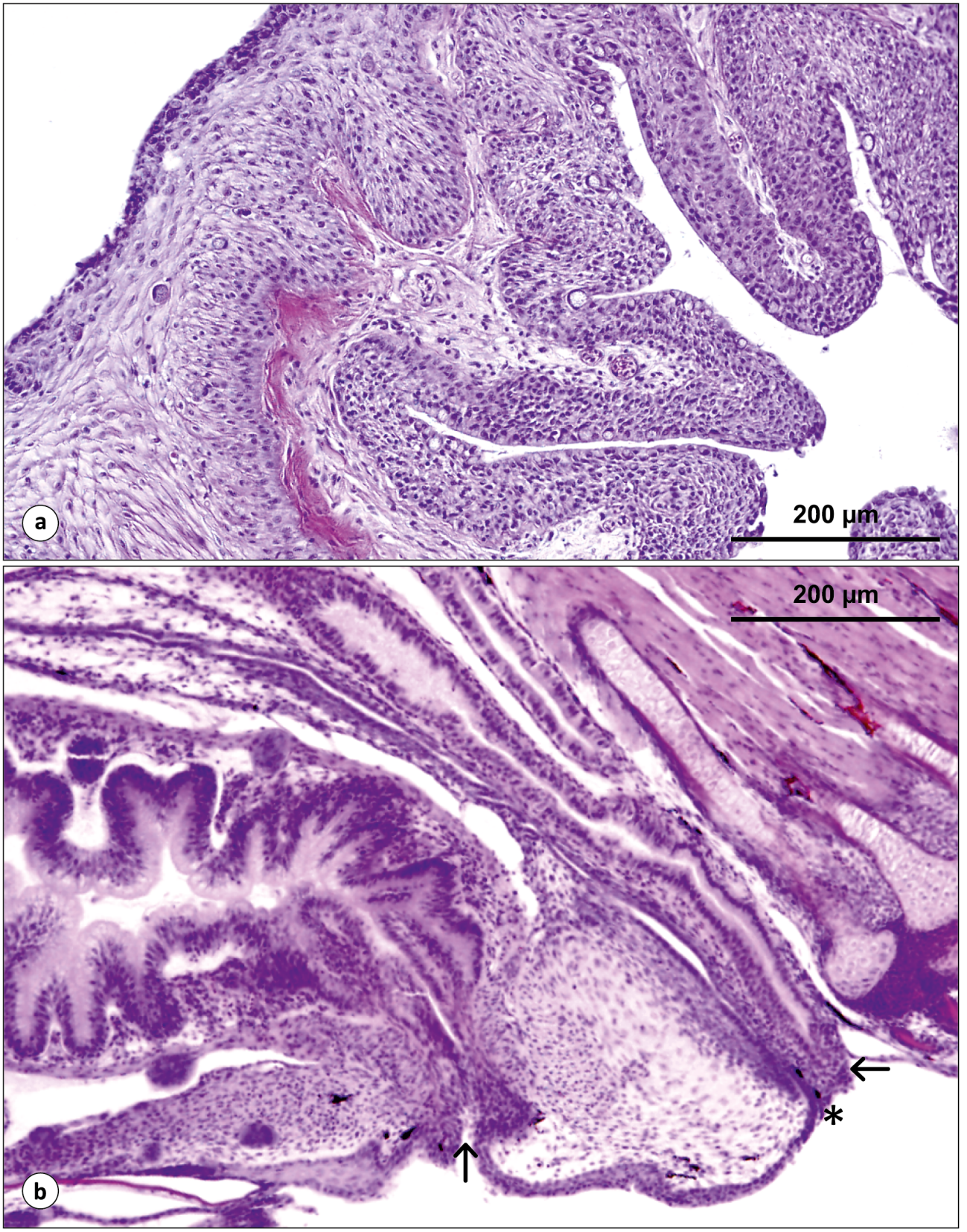

Fig. 9. Anal region. (a) Parasagittal section through anal region. Terminal orifice of alimentary tract (anus) is surrounded by anal papilla. Towards exterior, epithelium transforms gradually from the simple to the stratified type. (b) Digestive, reproductive, and urinary systems discharge separately. Genital orifice (*) lies posterior to anus (↑). Two urinary ducts unify immediately before their orifice positioned posterior to the genital orifice (←). Adult NF (a), adult NR (b).

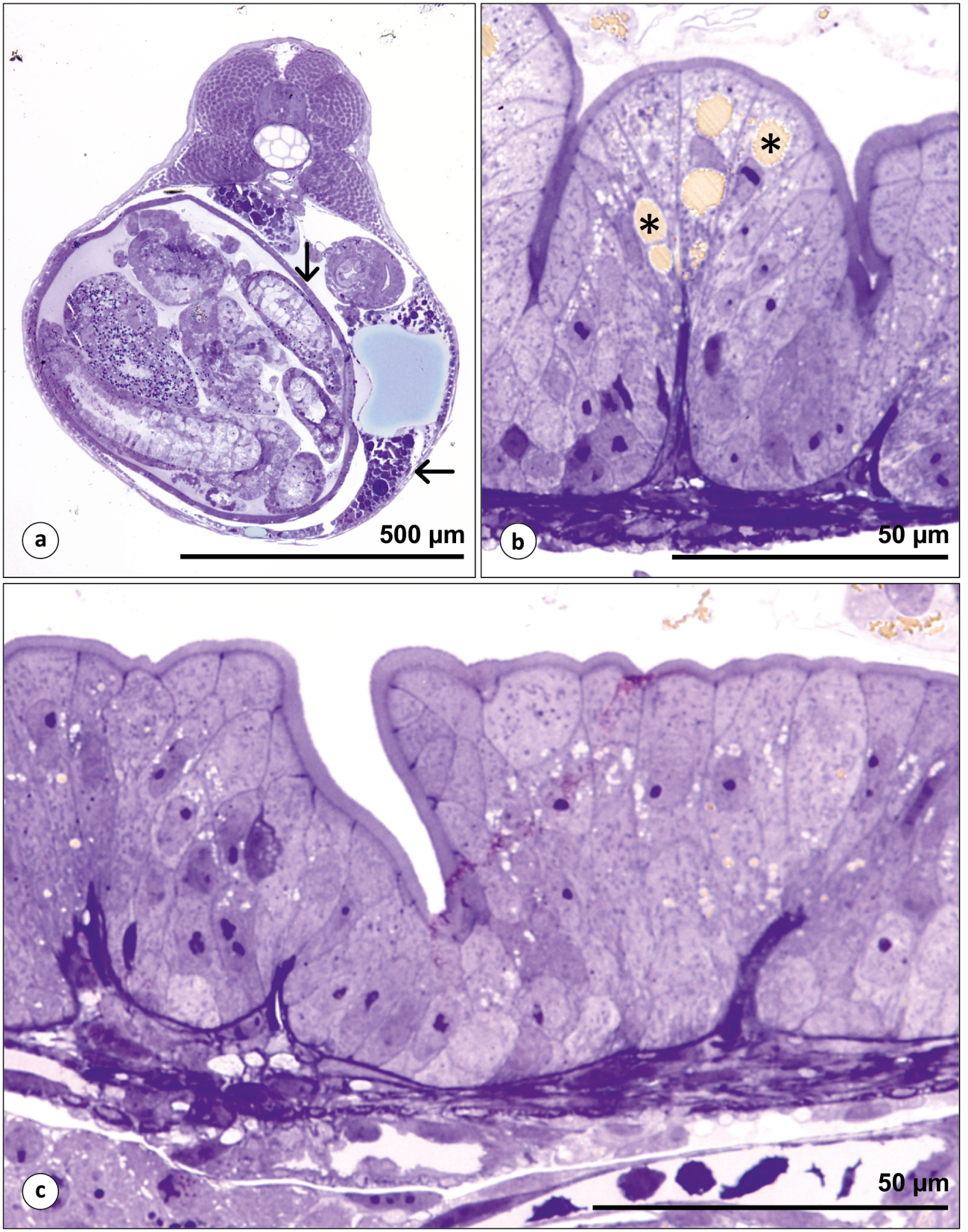

Fig. 10. Digestive tract of larval stages. Semi-thin sections. (a) Cross section through entire fish body at the level of midgut shows extremely distended digestive tube and the abdomen which contains remnants of yolk sac (←). A high food intake typical of this life cycle stage causes thinning of the intestinal wall (↓) and disappearance of mucosal folds. (b, c) Details of enterocytes with thick brush border and absorbed yolk rich in lipids (*). NF.

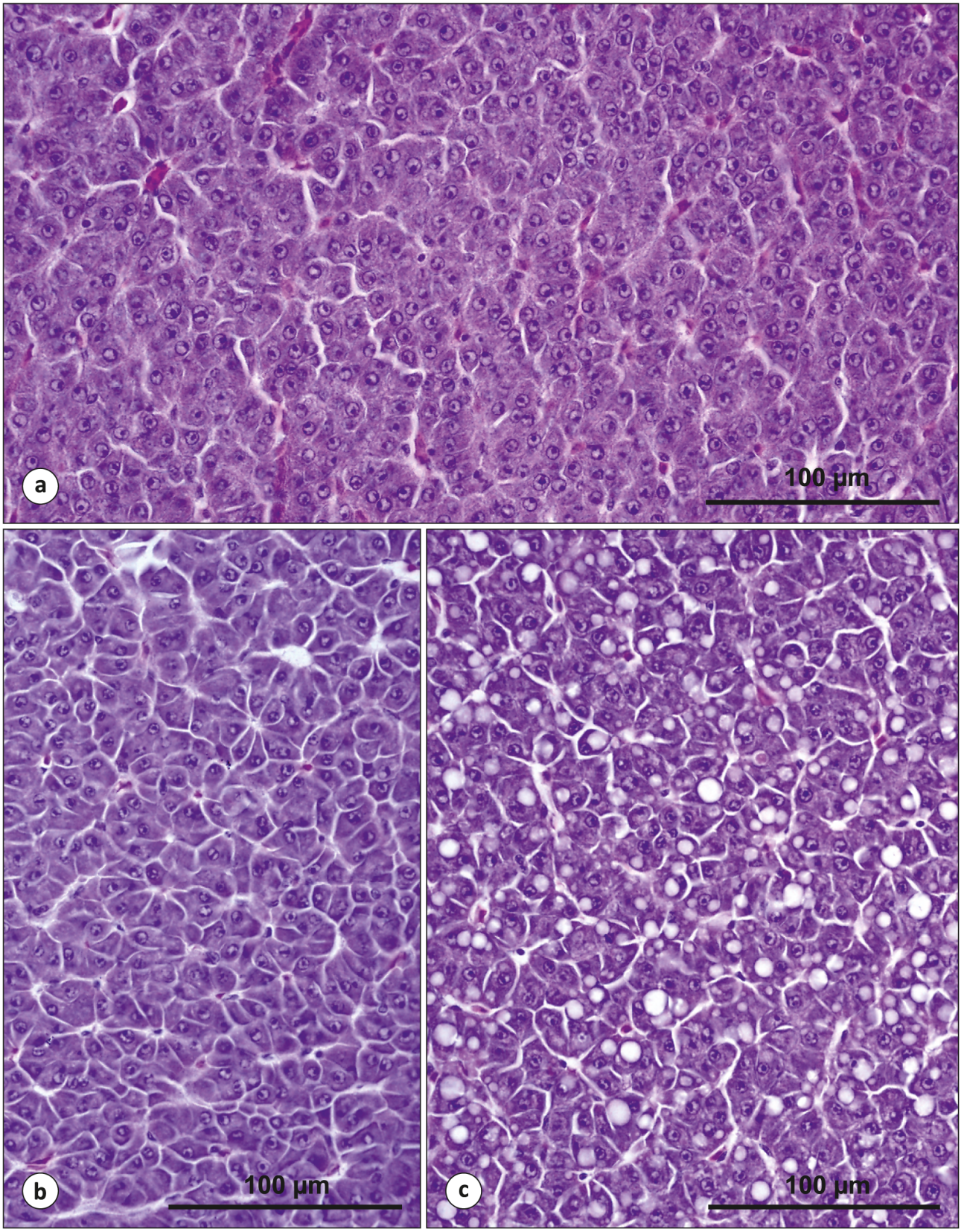

Fig. 11. Liver. Liver parenchyma of NF females collected in wild populations. Samples were taken and sectioned from left (parietal) side of the organ. (a, b) Sections show characteristic two-cell laminae of hepatic cords and absence of lobulation. (c) Sharply outlined, round vacuoles seen in hepatocytes stained with H&E are signs of lipid deposition (storage). Vacuoles are empty in material processed by conventional paraffin technique. Adult NF.

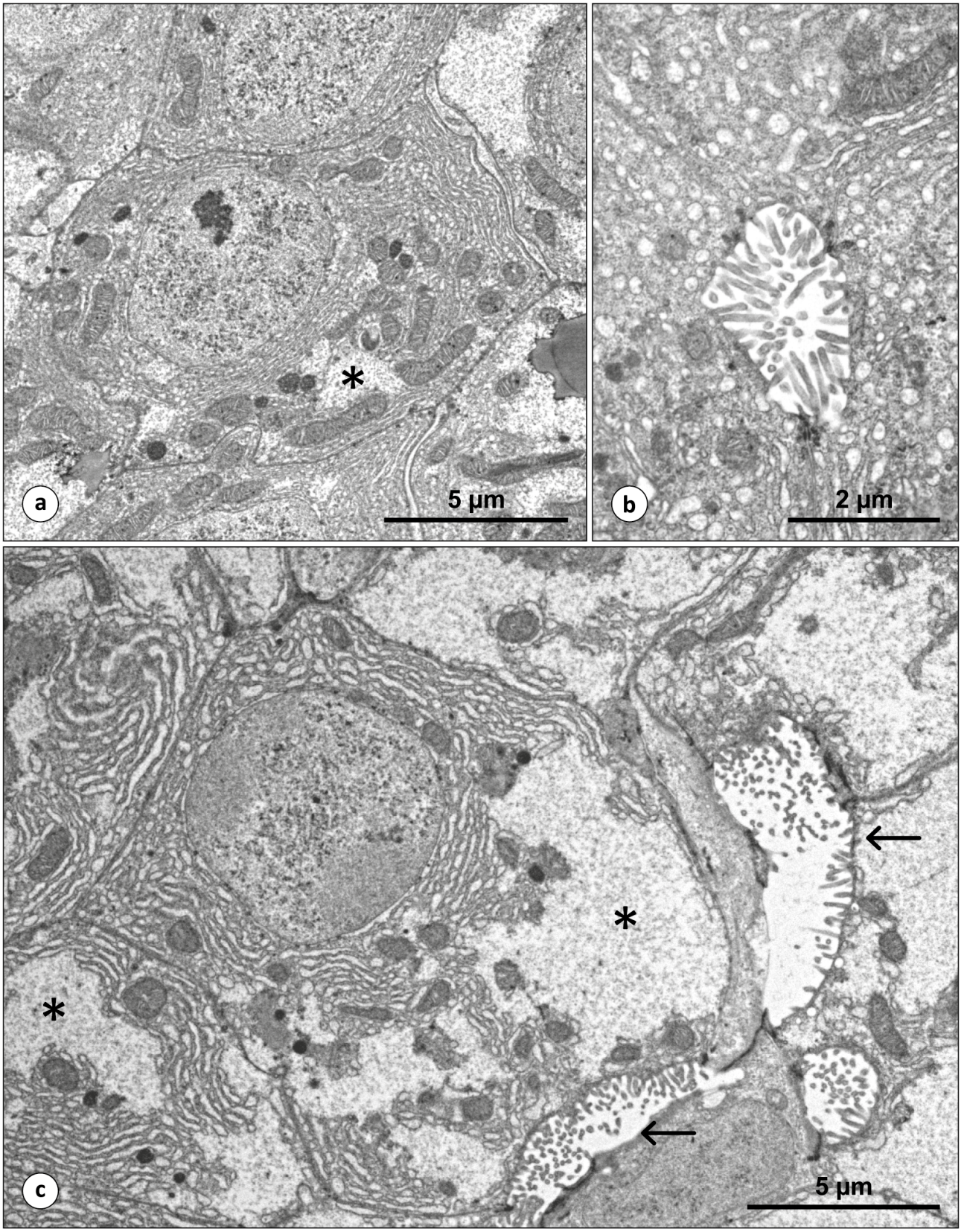

Fig. 12. Ultrastructure of liver parenchyma. (a) Hepatocyte of typical polyhedral shape with round euchromatic nucleus and electron dense nucleolus. Cytoplasm rich in RER contains multiple mitochondria and small electron lucent zone with deposit of glycogen (*). (b) Bile canaliculus among adjacent hepatocytes with microvilli projecting into its lumen. (c) Hepatocytes with prominent deposits of glycogen (*) and adjacent, obliquely sectioned bile canaliculi (←). Adult NF.

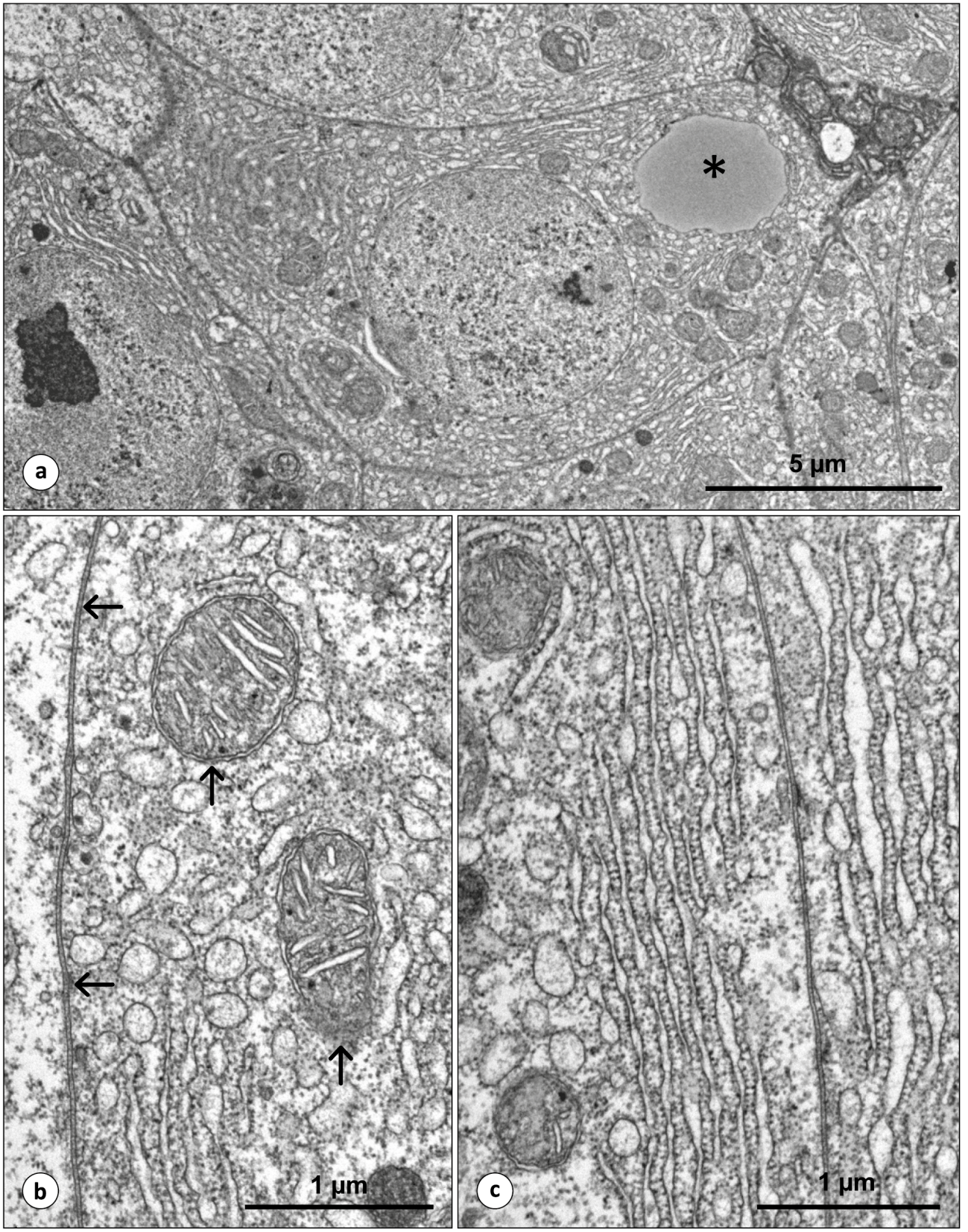

Fig. 13. Ultrastructure of hepatocytes. (a) Hepatocyte with prominent euchromatic nucleus and intracytoplasmic vacuole containing lipids (*). In size and electron density of content, the vacuole corresponds to the physiological (temporary) presence of fat. (b) Mitochondria (↑), cell membrane (←), vesicles of SER, and bundles of cisternae of RER that are better seen in (c), indicate good cell condition. Alterations of these cell organelles are mostly considered signs of cell aging. Adult NF.

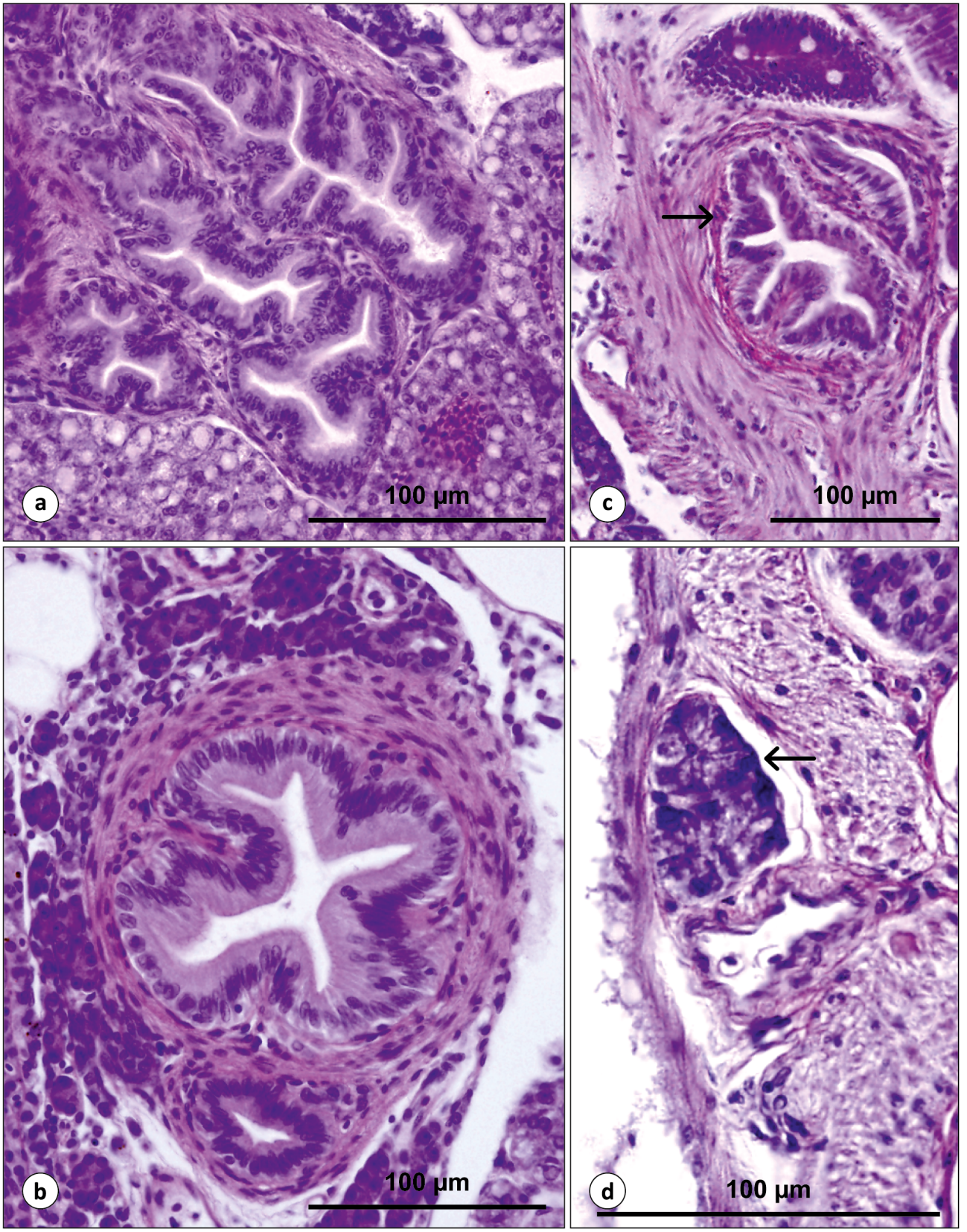

Fig. 14. Digestive gland ducts. Connection of the digestive tract associated glands that produce bile and secretions of exocrine pancreas with the gut is not easy to follow in histological sections, however details of importance were observed. (a, b) Bile ducts which transport bile into and from gall bladder, respectively. (c) Entrance of undetermined digestive gland duct into gut (→). (d) Small nodule of exocrine pancreas embedded in the wall of intestine (←). Adult NA (a), adult NF (b, c, d).

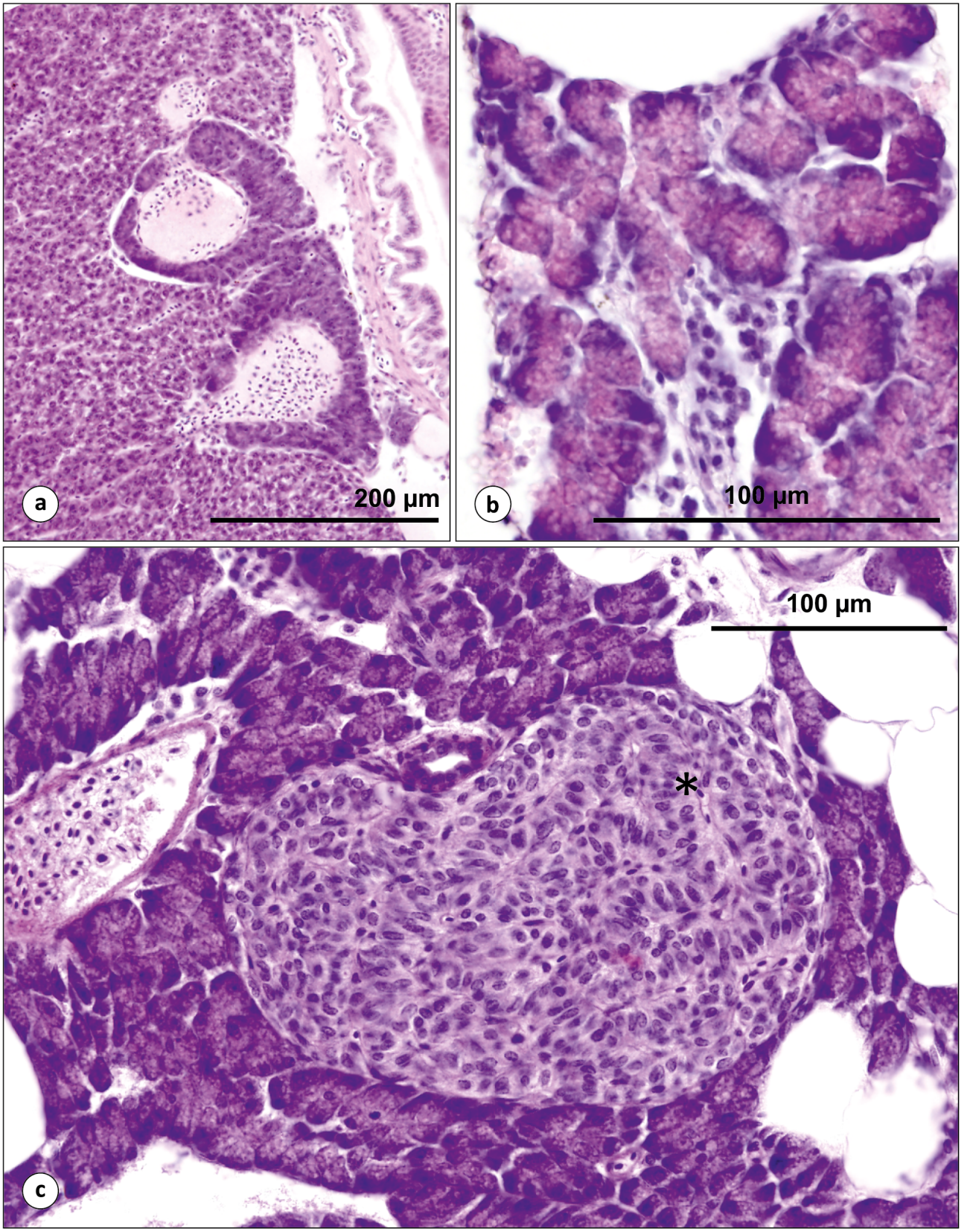

Fig. 15. Pancreas. (a) Pancreas, an important exo- and endocrine organ seen among other organs of the body cavity, while minor portion of this organ has intrahepatic localization. (b) Zymogen granules are the most characteristic feature of cell cytoplasm in exocrine pancreatic acini. (c) Islets of Langerhans (*) of endocrine pancreatic tissue surrounded by exocrine pancreatic tissue. Islets of Langerhans were only seen within extrahepatic exocrine acini. Adult NF.

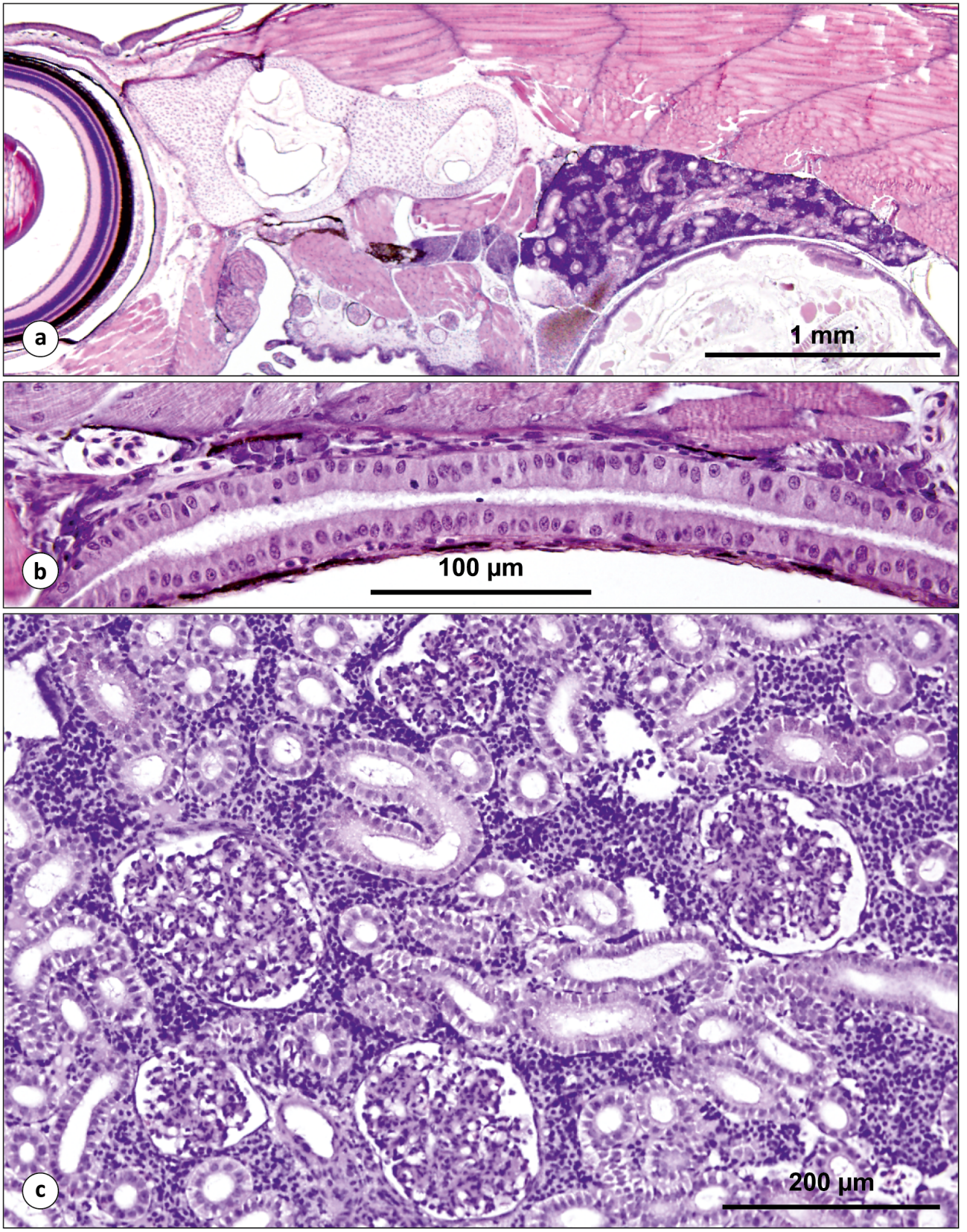

Fig. 16. Trunk/posterior/excretory kidney I. (a) Retroperitoneal position of kidney in the cephalic part of body seen in overview. (b) One of two long collecting/urinary ducts which run below the vertebral column throughout the whole of the body cavity. The paired ducts unify at the level of anal fin and discharge posterior to the genital orifice and anus. (c) Excretory part of kidney with nephrons interconnected with system of tubules and interstitial hemopoietic tissue. Juvenile (a) and adult (b, c) NF.

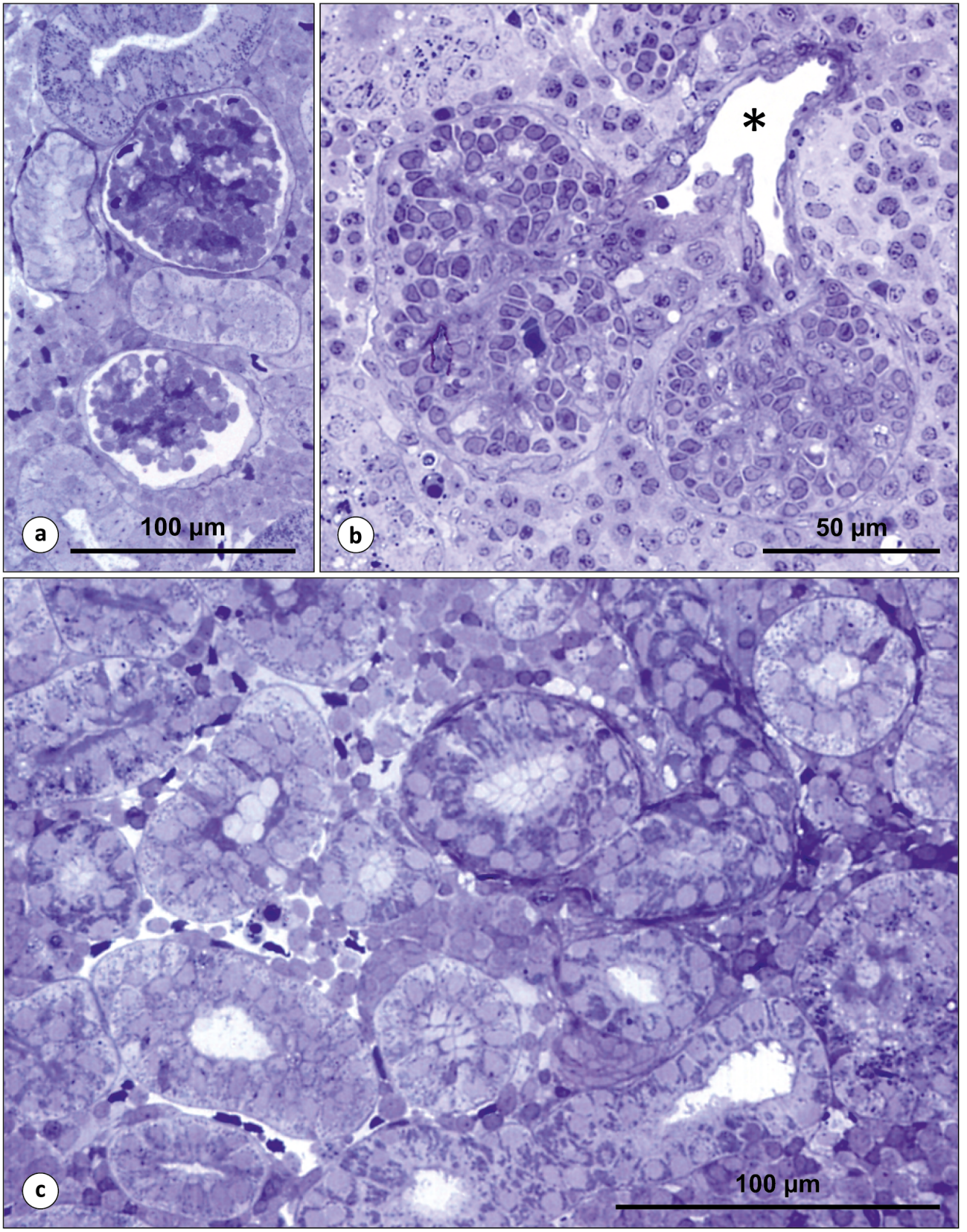

Fig. 17. Excretory kidney II. Main components of excretory kidney tissue seen in semi-thin sections. (a) Overview of two renal corpuscles with different-sized Bowman's spaces surrounded by convoluted tubules. (b) Pair of renal corpuscles, the urinary poles of which are confluent with lumen of proximal tubule (*). (c) Cross sections of convoluted tubules imply subcellular differences (hardly perceptible in paraffin embedded material) related to different segments of tubules. Adult NF.

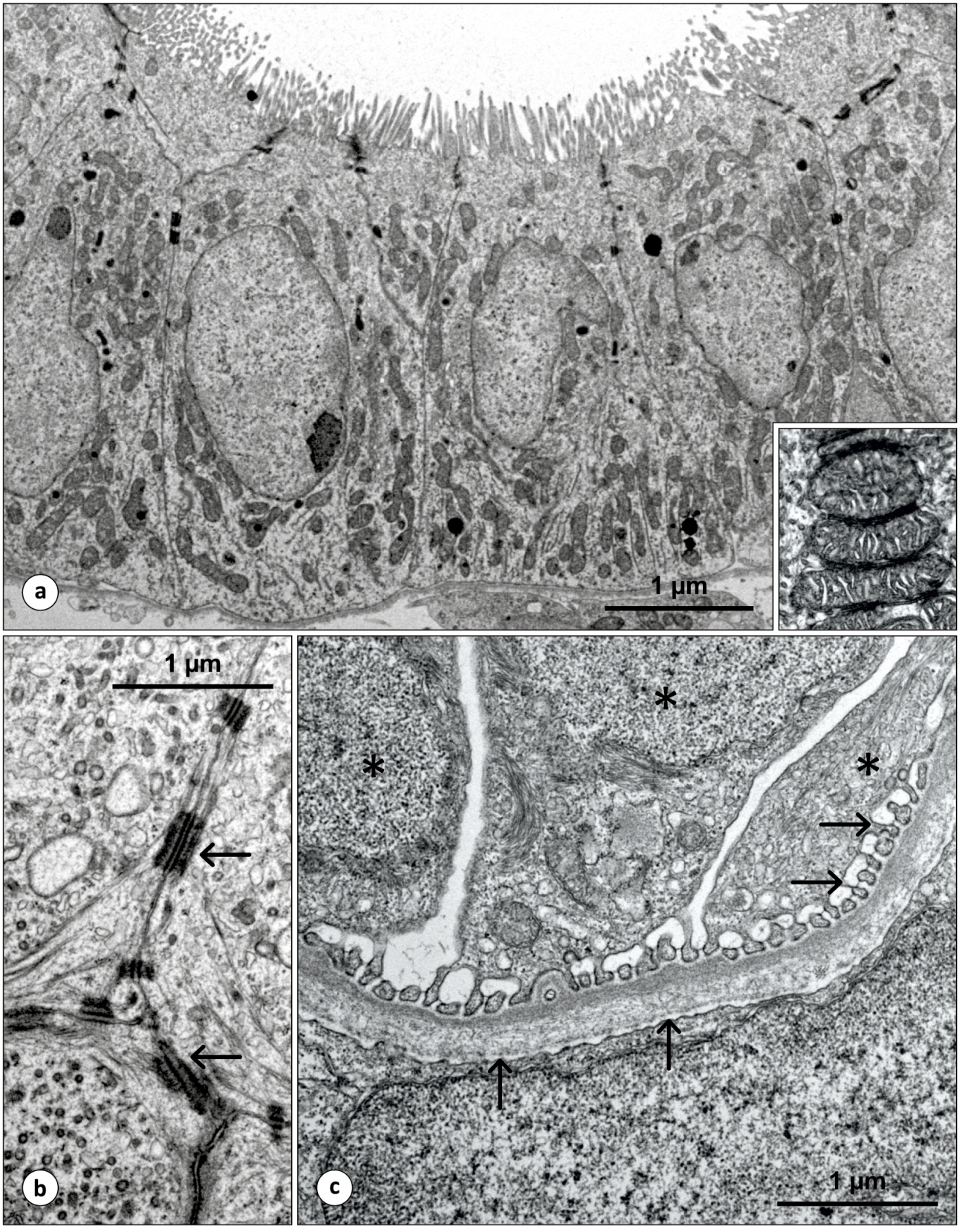

Fig. 18. Ultrastructure of excretory kidney. (a) Cuboidal cells of proximal convoluted tubule sectioned transversally. Cells display large nuclei, numerous mitochondria (see also inset), and long apical microvilli. (b) Intercellular junctions of epithelial cells closely resemble desmosomes (←). (c) Part of a renal corpuscle covered with visceral layer of Bowman's capsule. Podocytes (*) with basal membrane (↑) and pedicels (→) are constituents of blood filtration barrier. NF.

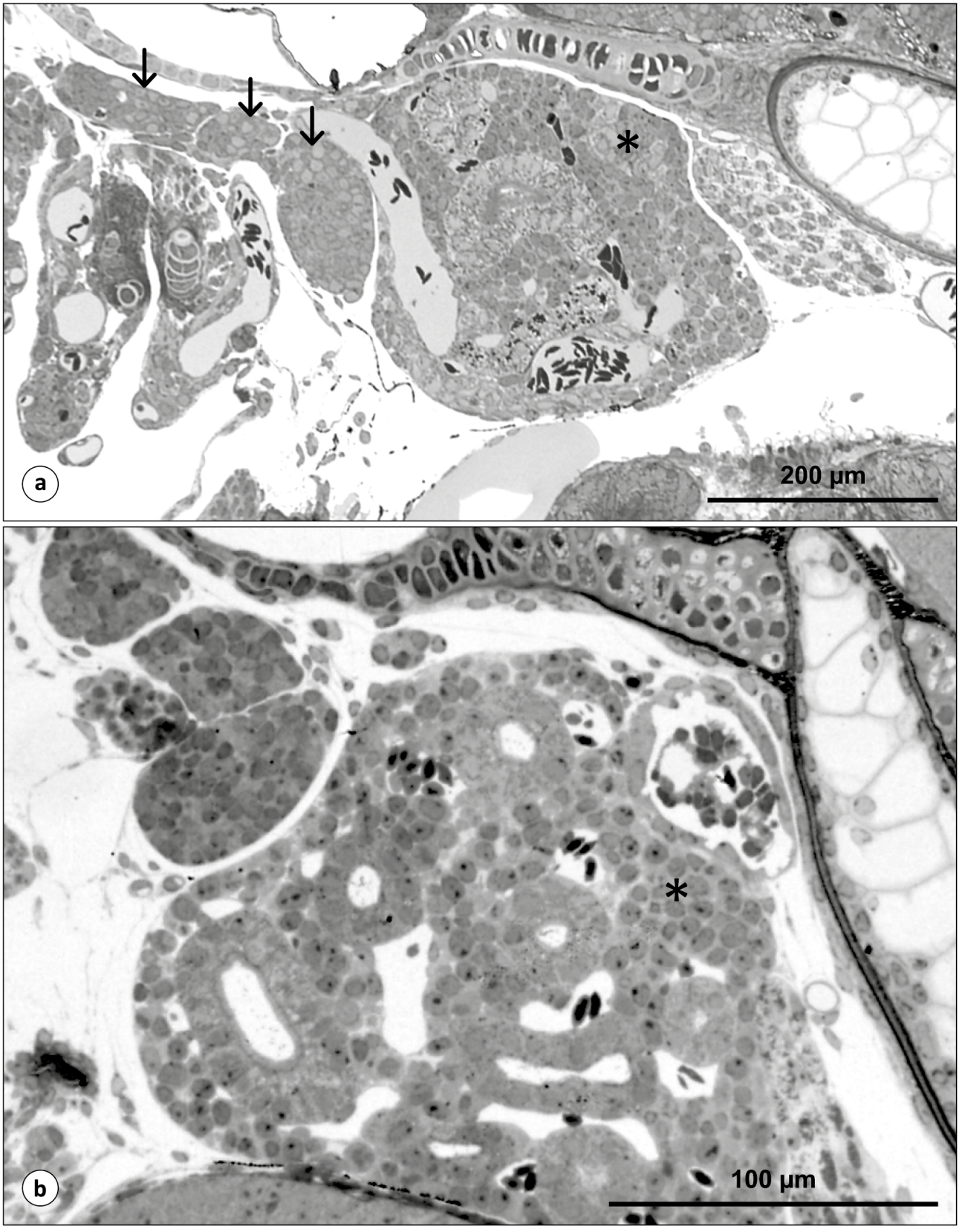

Fig. 19. Larval kidney. (a) Parasagittal section through cephalic region of NF fixed 24 hph demonstrates localization of head/hemopoietic kidney (↓) between branchial cavity and the base of the skull. Voluminous trunk/excretory kidney (*) adjoins caudally. (b) The structure of hemopoietic interstitial tissue in trunk kidney (*) shown in detail. The renal topography (identical in adults) poses sampling difficulties and is a source of inaccuracies in recognition of renal segments. NF.

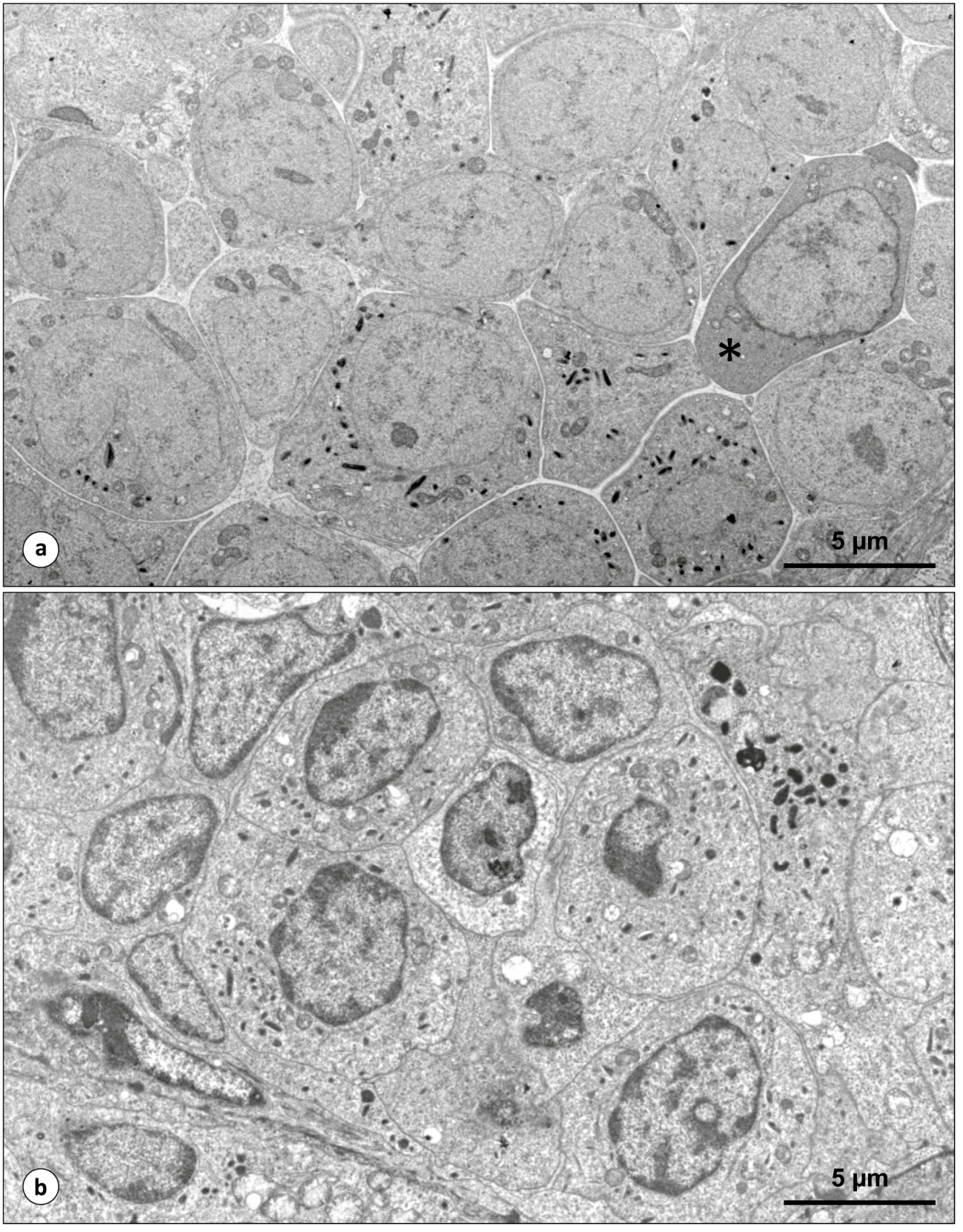

Fig. 20. Hemopoietic kidney tissue. (a) Intertubular/interstitial tissue consists of mononuclear haemoblasts with nuclei that contain loosely arranged euchromatin. Nuclear chromatin is slightly peripheral in one erythroblast (*). (b) Precursors of monocytes seen in advanced stage of haematopoiesis contain dark/electron dense areas of compact heterochromatin usually apposed to nuclear envelope. Cytoplasmic granules do not differ substantially from less differentiated blasts in (a). Larval NF.

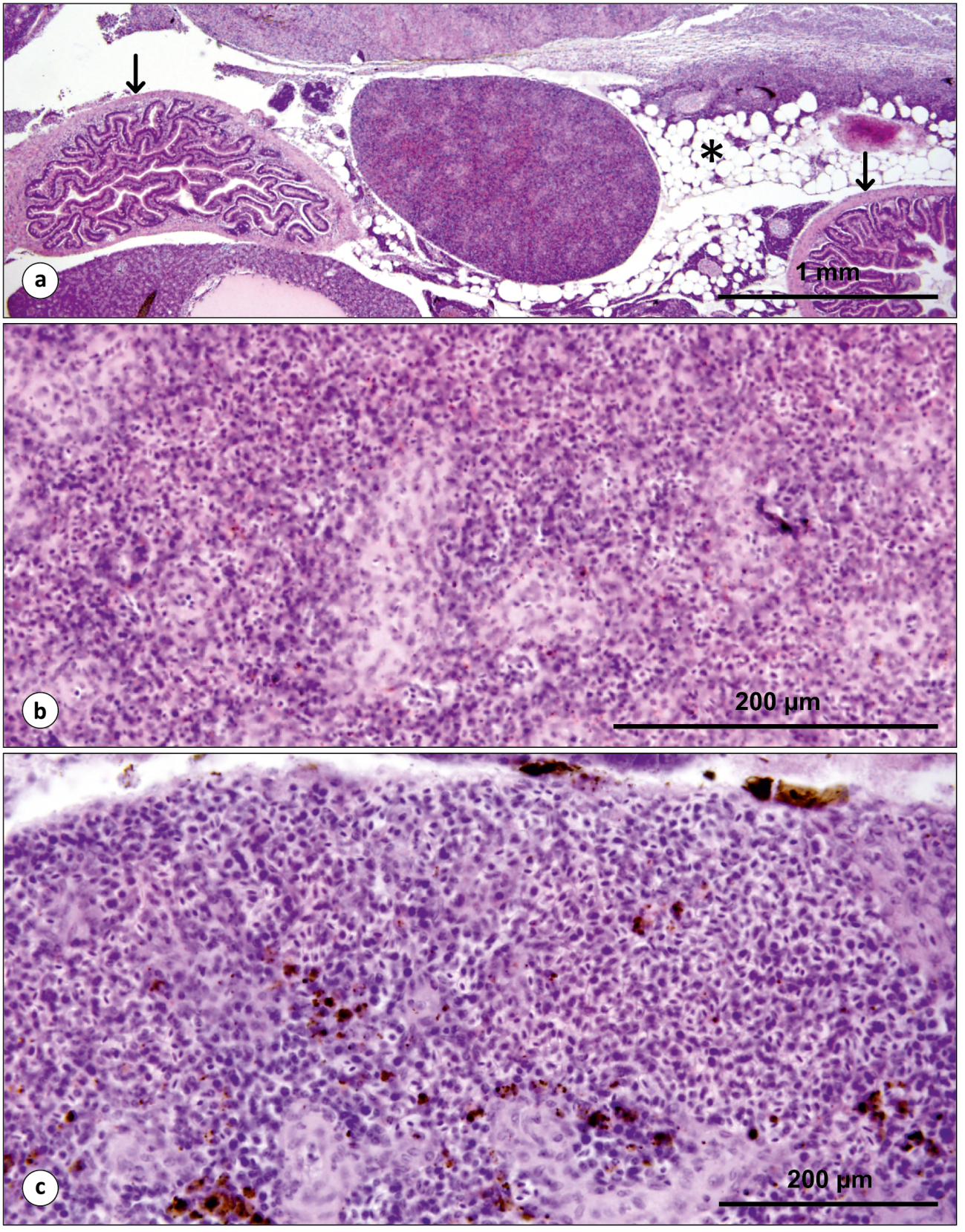

Fig. 21. Spleen I. (a) Spleen situated in body cavity close to the liver and two segments of midgut (↓), and surrounded by fat tissue (*). (b) An overview of spleen parenchyma with indistinct connective tissue framework and ellipsoids, and diffuse, indistinct differentiation of red from white pulp. (c) Periphery of spleen contains numerous erythroid cells, while capsule is very thin. The presence of dark pigment aggregates is associated with blood cell destruction. Adult NF.

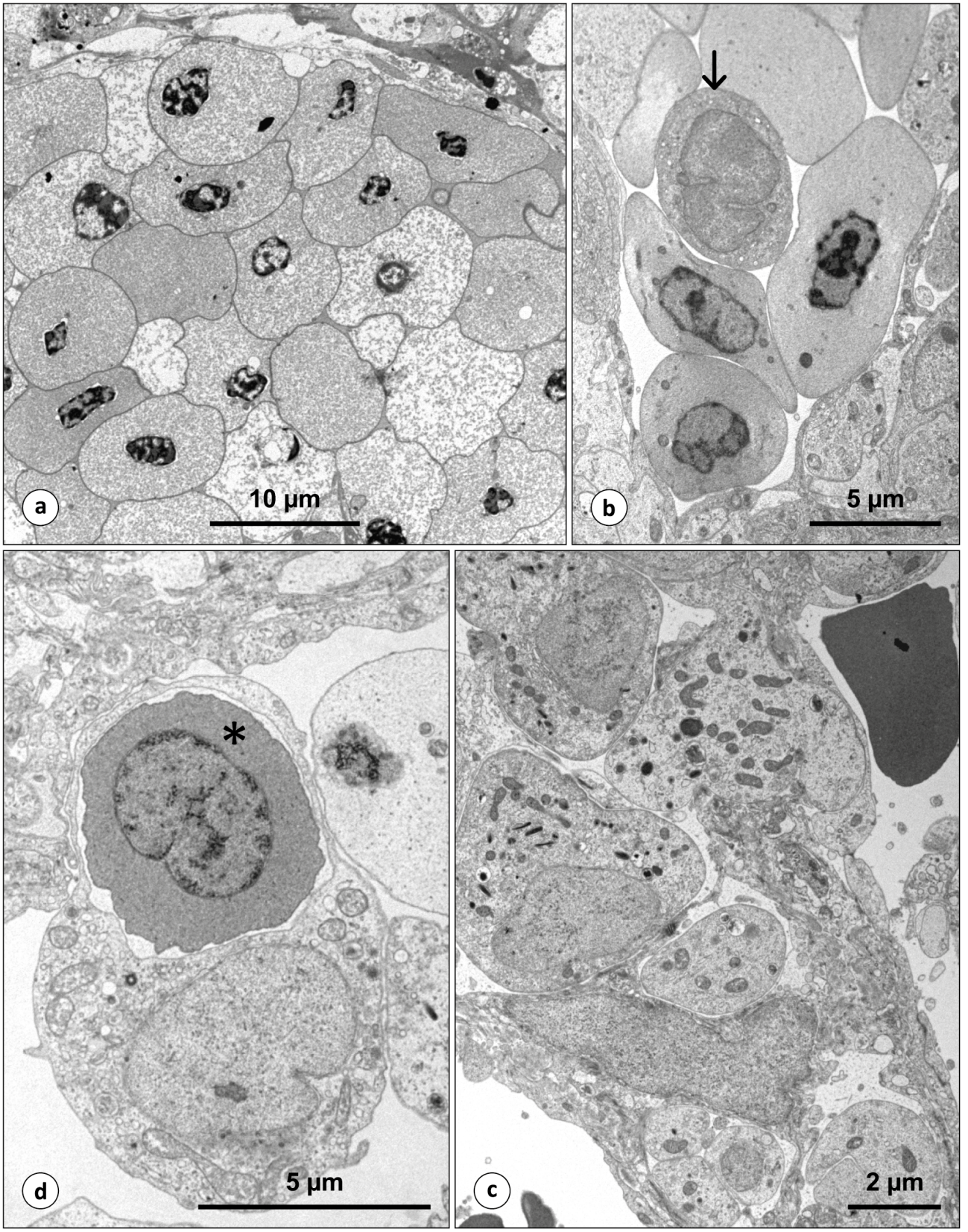

Fig. 22. Spleen II. (a) Aggregate of erythroid cells concentrated in red pulp, the main part of spleen parenchyma responsible for erythropoiesis. Individual cells differ in content of cytoplasmic haemoglobin. (b) Erythrocytes and haemoblast (↓), multipotential blood cell precursor located in splenic sinusoid. (c) Hemoblasts predominating in white pulp. (d) Example of erythrophagocytosis (*) manifests an important role of spleen. Adult NF.

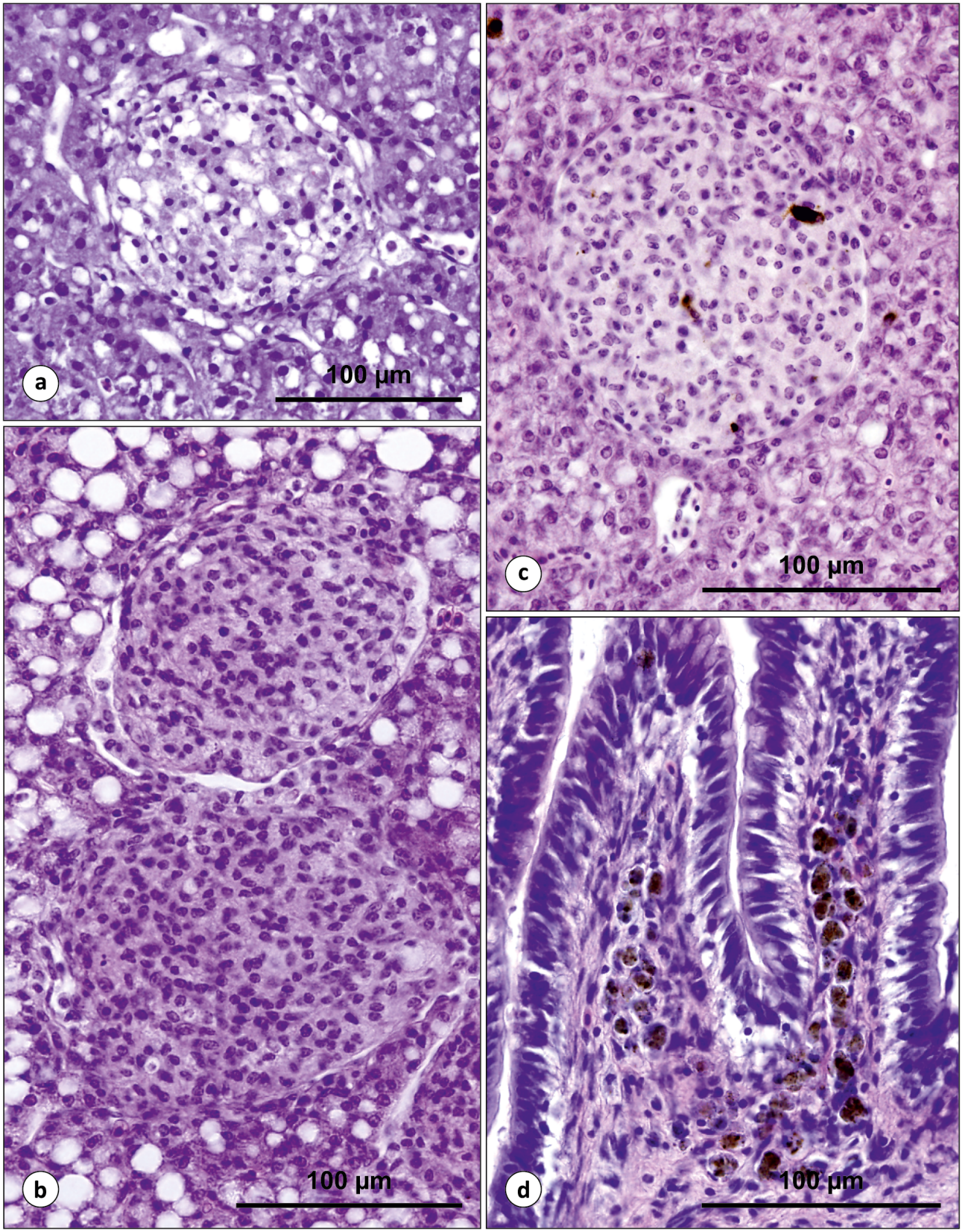

Fig. 23. Macrophage centres, also known as melanomacrophage centres. (a, b) Aggregates of mononuclear cells in the liver of two different *Nothobranchius* spp. Low magnification and H&E staining do not display more than the size uniformity of nuclei and delicate demarcation from surrounding tissue. (c) Melanomacrophage centre with small amount of dark pigment. (d) Darkly pigmented melanomacrophages seen in subepithelial tissue of the intestine. Adult NE (a), senescent (b) and adult (c) NF, adult NG (d).

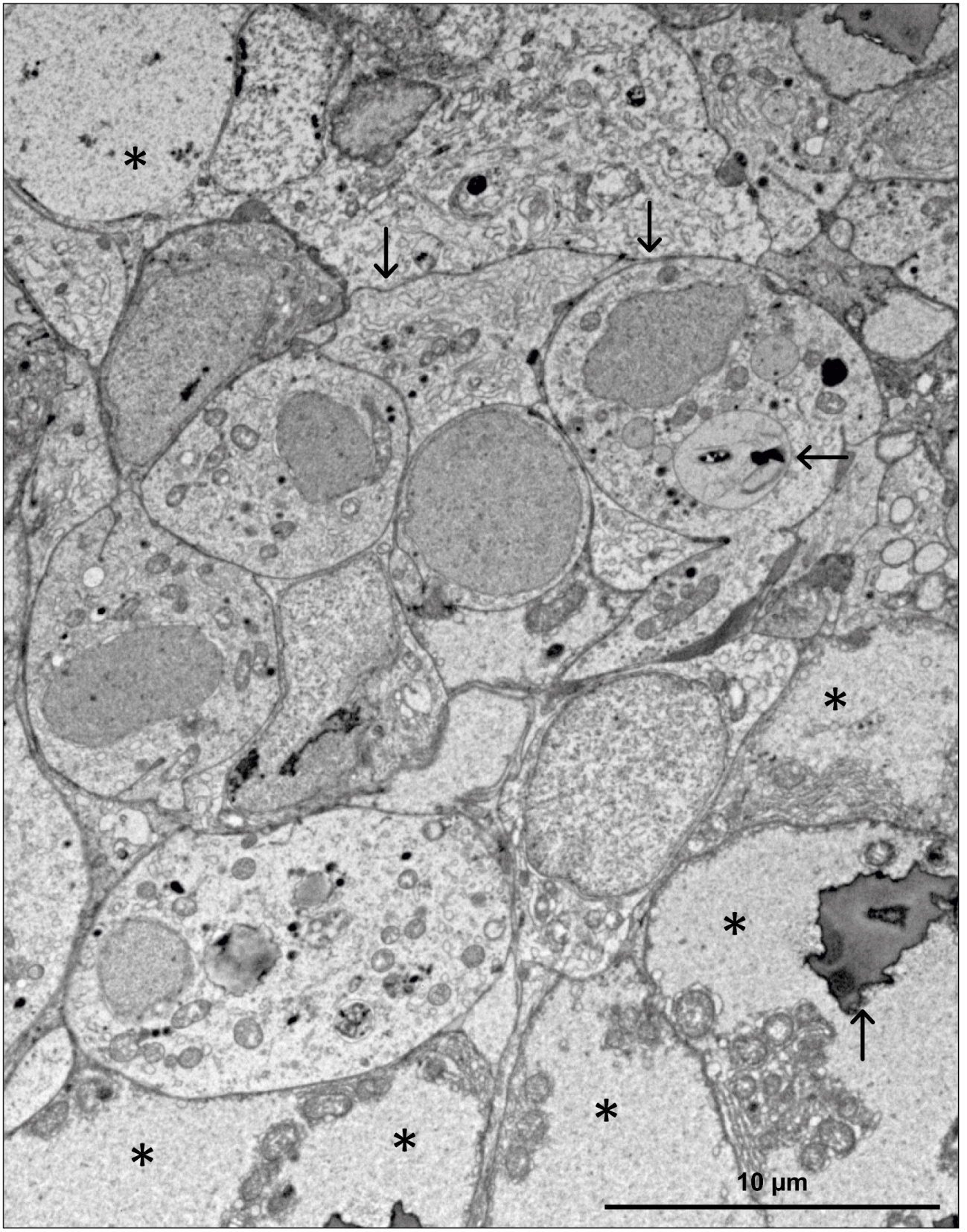

Fig. 24. Mononuclear cell aggregate (MA). Electron micrograph of small mononuclear cell aggregate (↓), component of fish mononuclear phagocytic system (MPS). Hepatocytes surrounding MA contain deposits of glycogen (*) and lipids (↑). Cytoplasmic phagosome (←) in one cell of the aggregate contains phagocytosed bacteria, which clearly assigns MA to mononuclear phagocyte system (MPS). Adult NF.

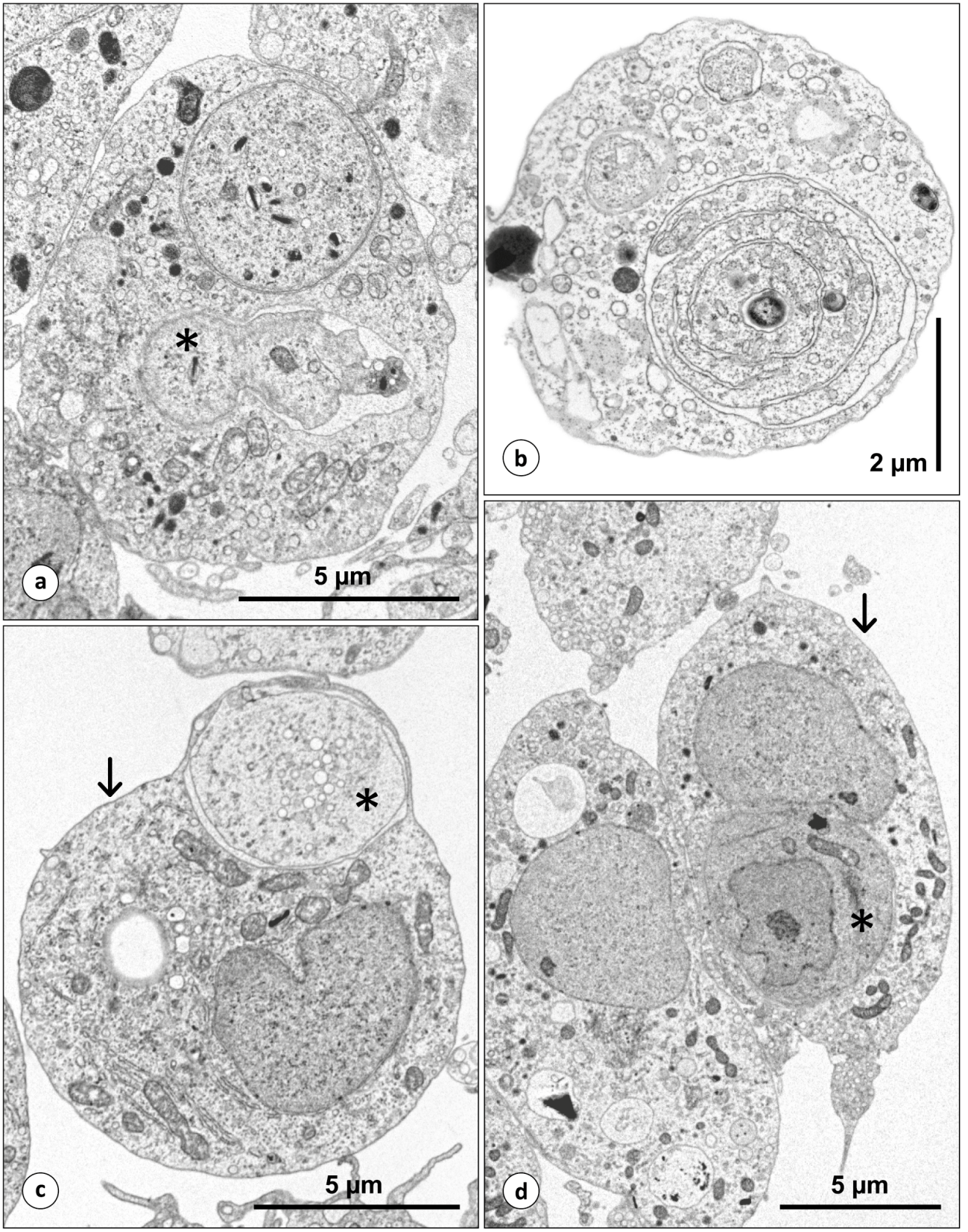

Fig. 25. Cells of mononuclear phagocyte system (MPS) I. Macrophages containing engulfed foreign particles (bacteria or eukaryotes) can be found in most organs and tissues. (a) Mononuclear phagocytic cell in liver with engulfed eukaryotic cell (*). (b) Example of specific, so-called coiling type of phagocytosis, known from bacterial infections. (c, d) Mononuclear phagocytes from spleen (↓), with engulfed eukaryotic cells (*). Adult NF.

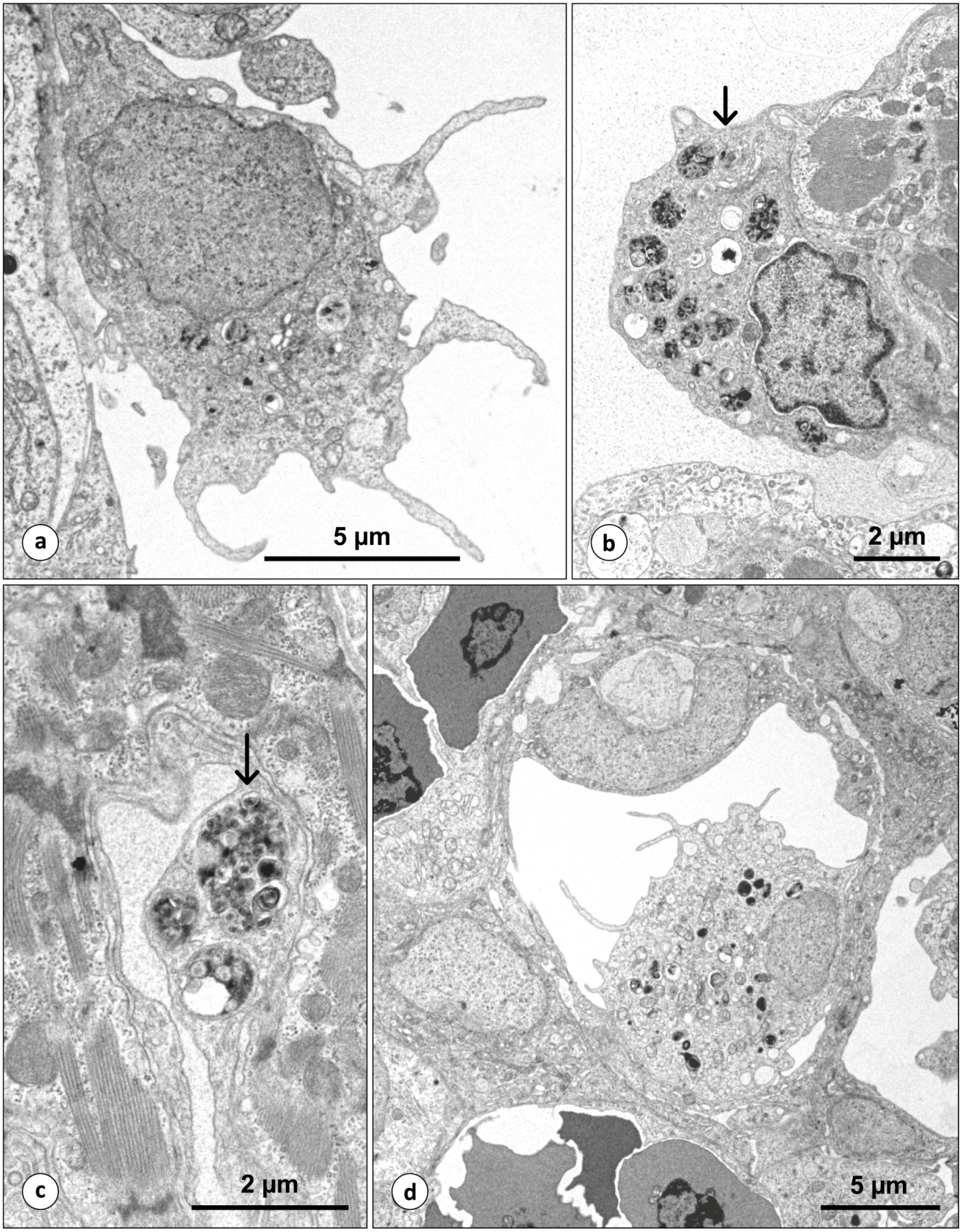

Fig. 26. Cells of mononuclear phagocyte system (MPS) II. (a) Protrusions emanating from the cell body, the type of nucleus, and cytoplasmic granules, match with morphological features of dendritic cells, which together with monocytes and macrophages are components of MPS. (b, c) Endothelial cells (↓) in heart capillary and endocardium respectively are "non-professional" phagocytes. (d) Both these types of cells seen in a section of spleen capillary. Adult NF.

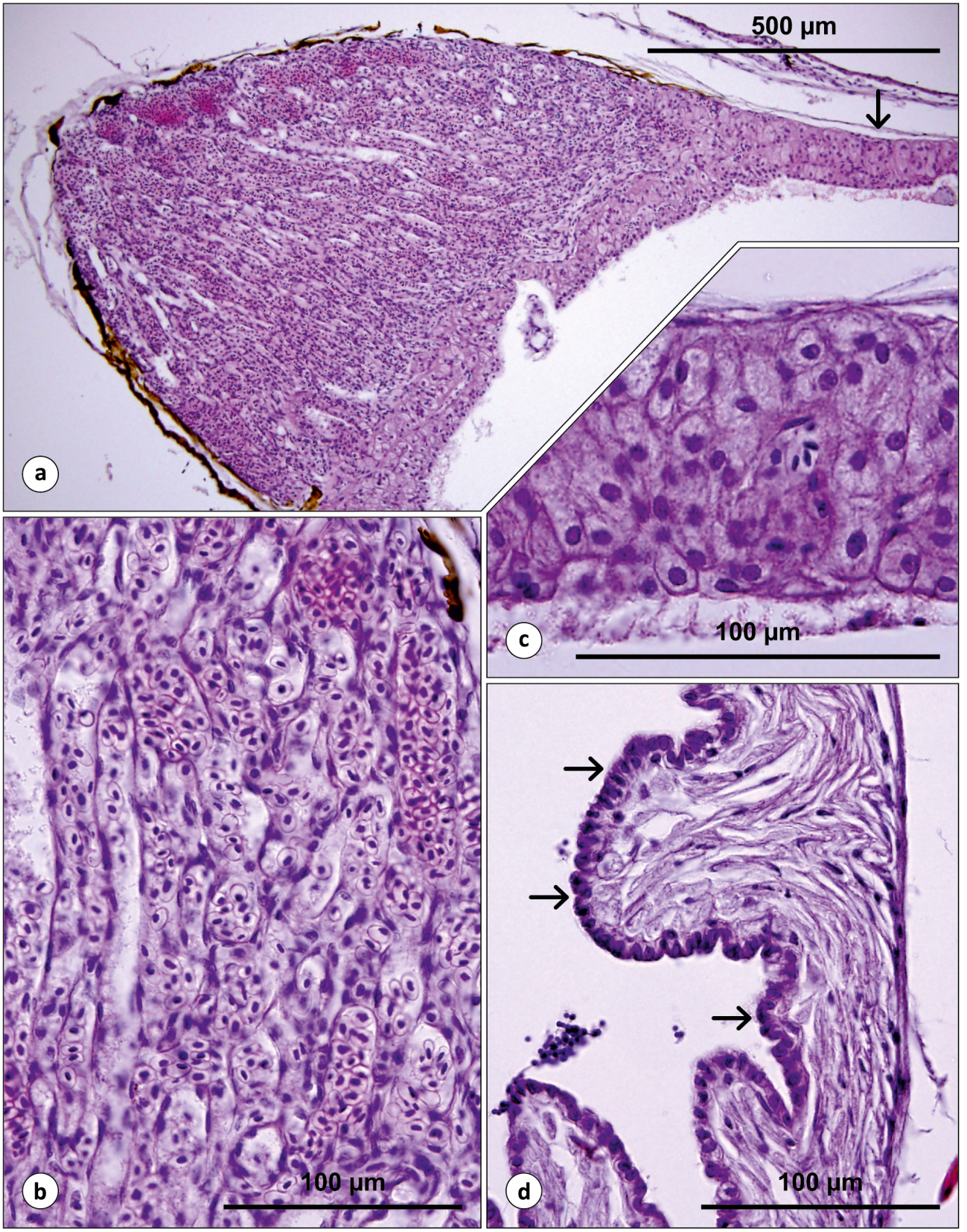

Fig. 27. Swim/gas/air bladder I. (a) Thick walled anterior part of swim bladder closely associated with capillary network/rete mirabile. (b) Detail of capillary network. (c) Detail of thick epithelial layer formed by secretory/resorbing cells corresponds to segment (↓) marked in (a). (d) Caudal/posterior part of swim bladder differs from anterior in structure and thickness of wall. Connective tissue of the wall is covered by simple cuboidal epithelium (→). Juvenile NF.

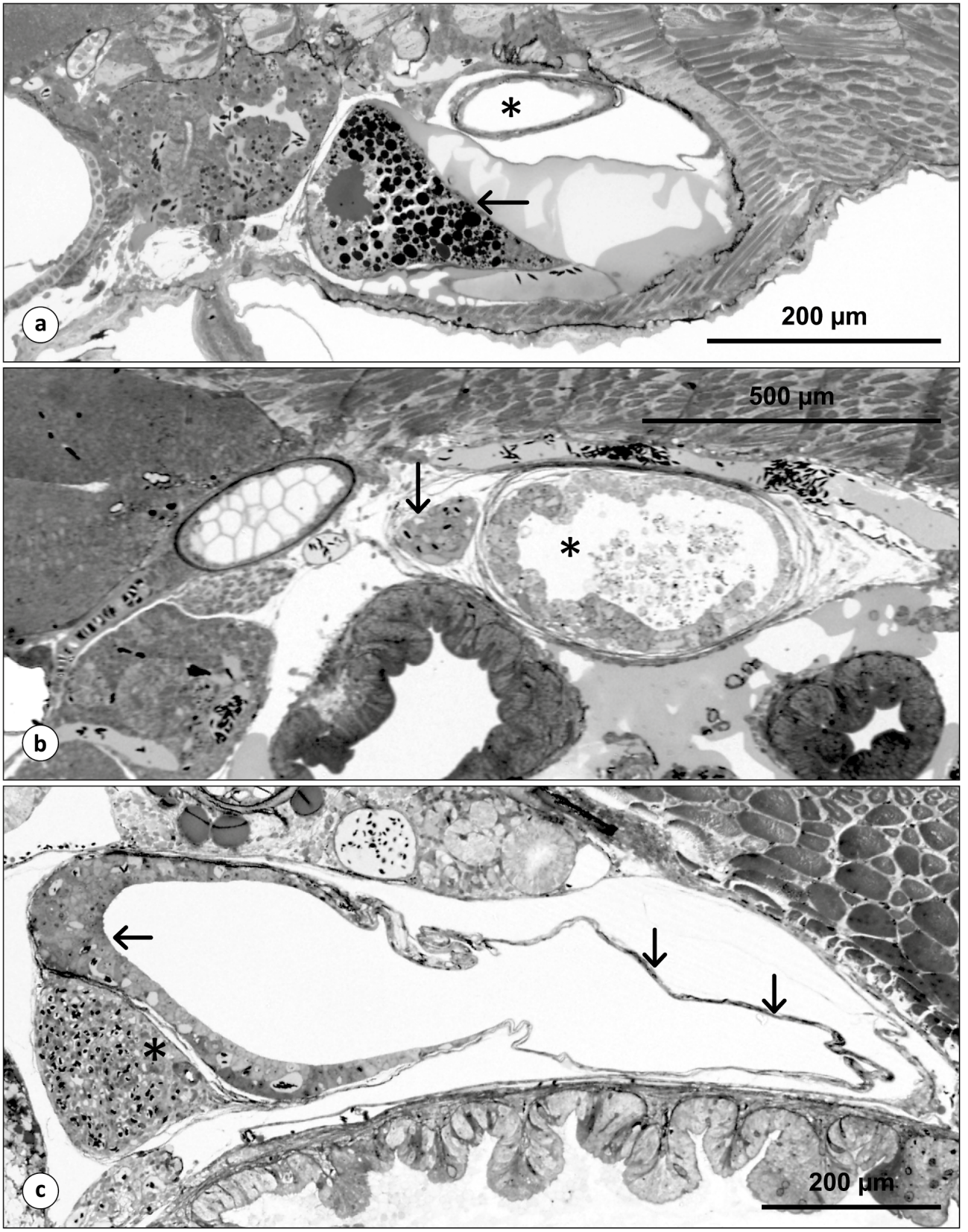

Fig. 28. Swim/gas/air bladder II. (a) Swim bladder (*) in larval stage 8 hph with barely identifiable structure, seen above remnants of yolk sack (←). (b) Larvae fixed 24 hph had a well-developed swim bladder (*) with secretory/resorbing epithelium and vascular rete mirabile in front of bladder (↓). (c) Swim bladder of 11-day-old individual was thick-walled anteriorly (←), where apposed to rete mirabile (*), and thin-walled (↓) posteriorly. NF.

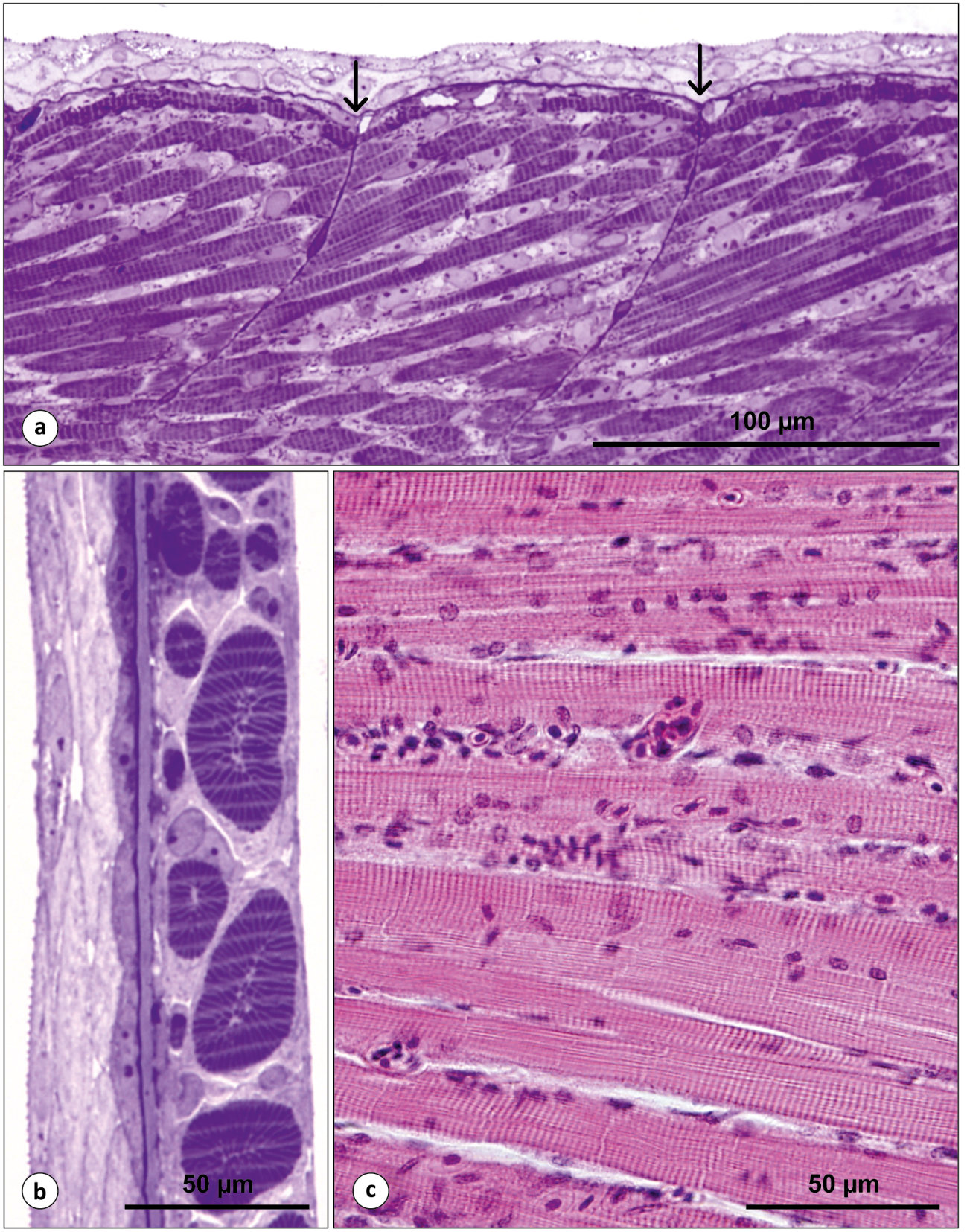

Fig. 29. Skeletal/striated muscles. (a) Longitudinal semi-thin section of NF fixed 24 hph. Myomeres of musculus latero-dorsalis arranged side-by-side along the body are separated by connective tissue myosepta (↓). Skin composed of thin layers of epidermis (stratified epithelium) and thin corium covers muscle tissue. (b) Transverse semi-thin section through body wall demonstrating myofibres at 24 hph. (c) Skeletal muscle of adult NF in paraffin section stained with H&E. NF.

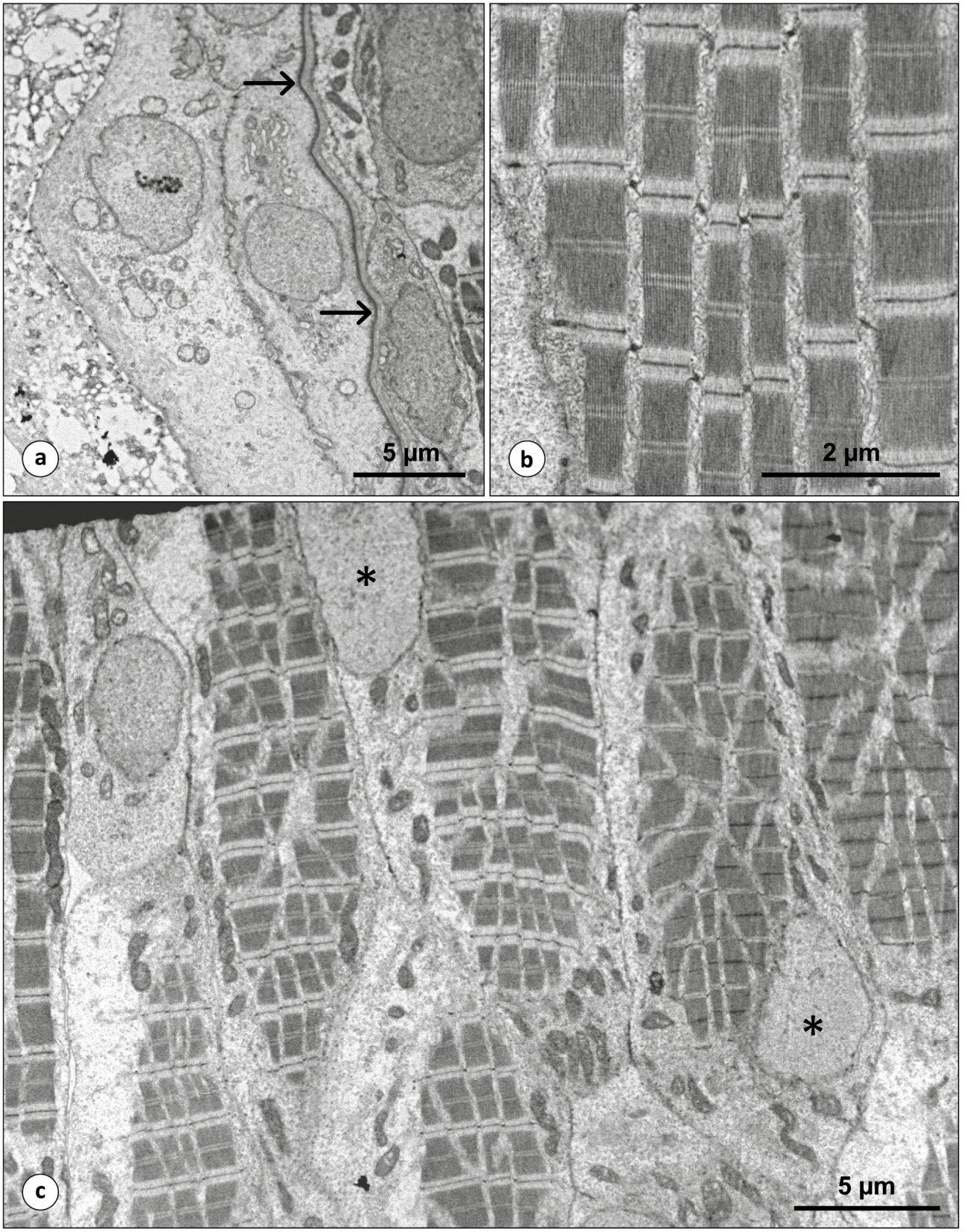

Fig. 30. Ultrastructure of skeletal muscles. (a) Subepidermal muscle tissue covered with epimysium (→) and skin epithelial cells on periphery. (b) Skeletal muscle fibre in longitudinal section. Sarcoplasm is packed with dark and light bands of myofibrils formed by cylindrical bundles of myofilaments. (c) Muscle fibres are multinucleated; the nuclei (*) occupy cell periphery close to sarcolemma with long axis parallel to that of the cell. NF.

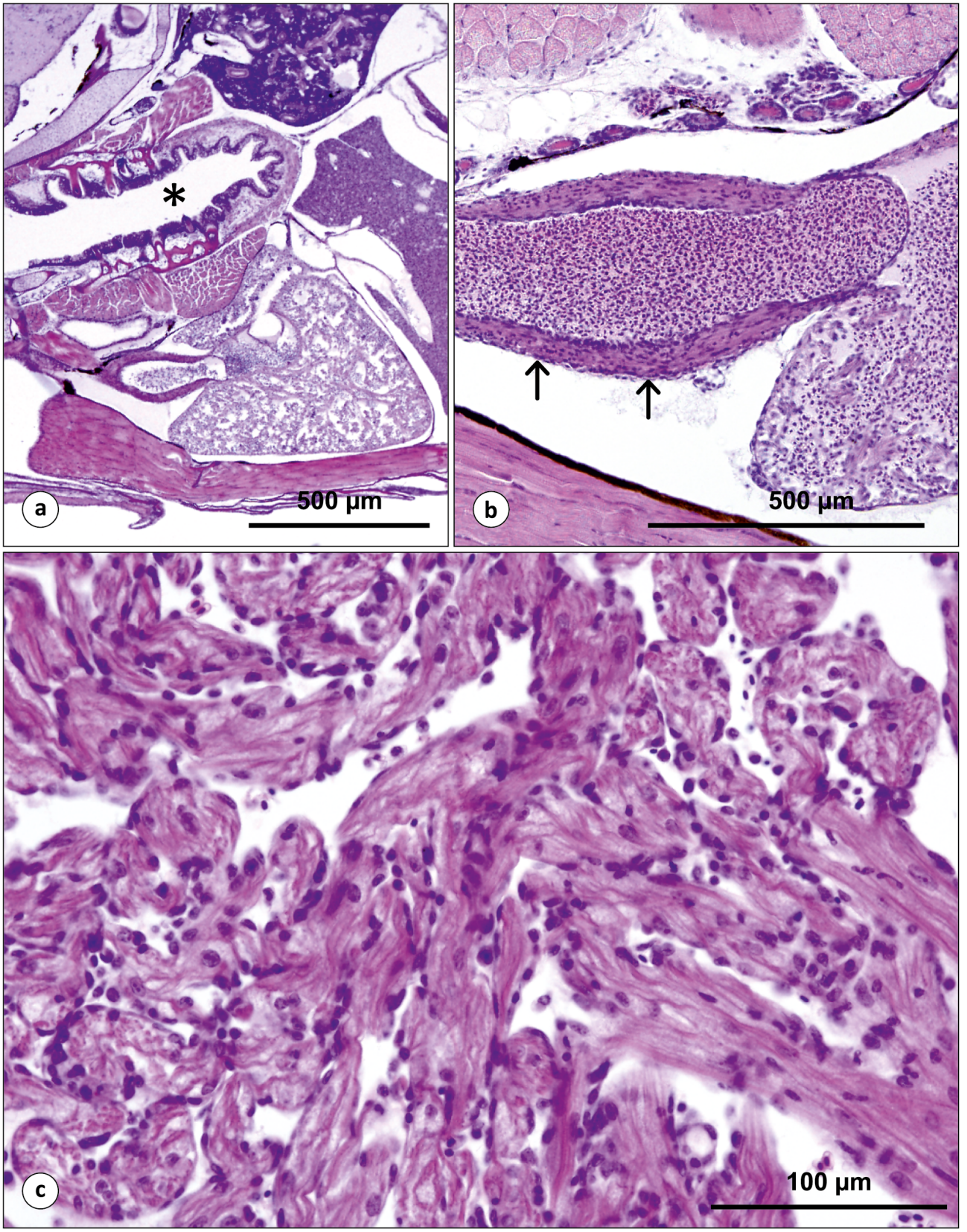

Fig. 31. Heart. (a) Localization of heart in an anterior part of fish body, in close vicinity of ventral body wall, pharyngeal part of headgut (*) and liver. (b) Bulbus arteriosus with thick wall composed of connective tissue containing elastic fibres (↑) and lumen filled with blood. Part of ventricle is also seen in this section. (c) Cardiac muscle fibres bifurcate and connect with each other, forming three-dimensional network covered with endocardial endothelium. NE (a), NR (b), NF (c).

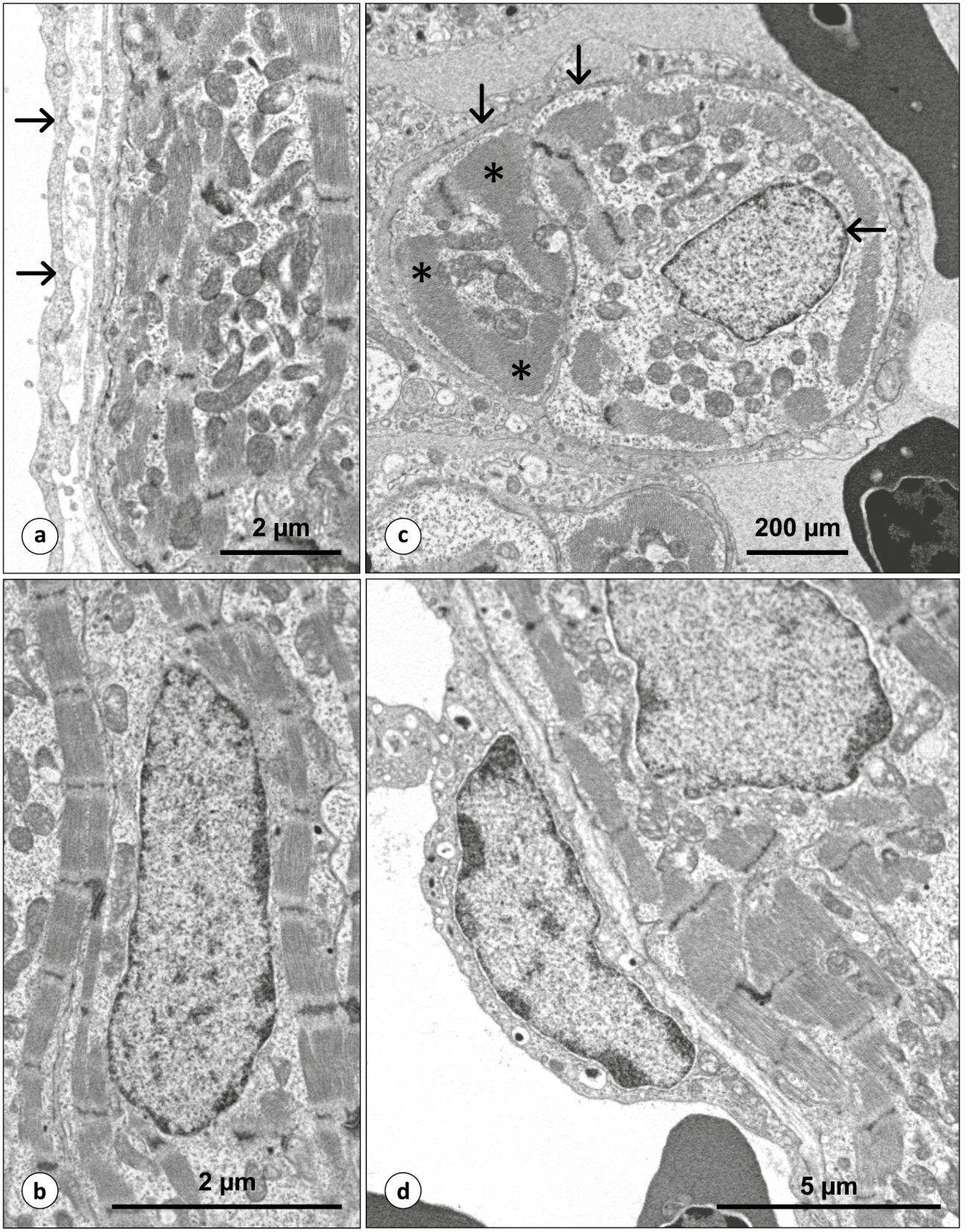

Fig. 32. Ultrastructure of cardiac muscle formed by muscle fibres (myocardial cells or myocytes). (a) Thin outer epicardium and narrow pericardial cavity (→), sarcolemma and part of myocyte with myofibrils and numerous mitochondria. (b) Longitudinal section shows central position of an ovoid nucleus and branching myofibrils. (c) Transverse section of muscle fibre with nucleus (←), mitochondria, myofibrils (*) and lamina externa (↓) covering sarcolemma. (d) Endothelial cell of endocardium. NF.

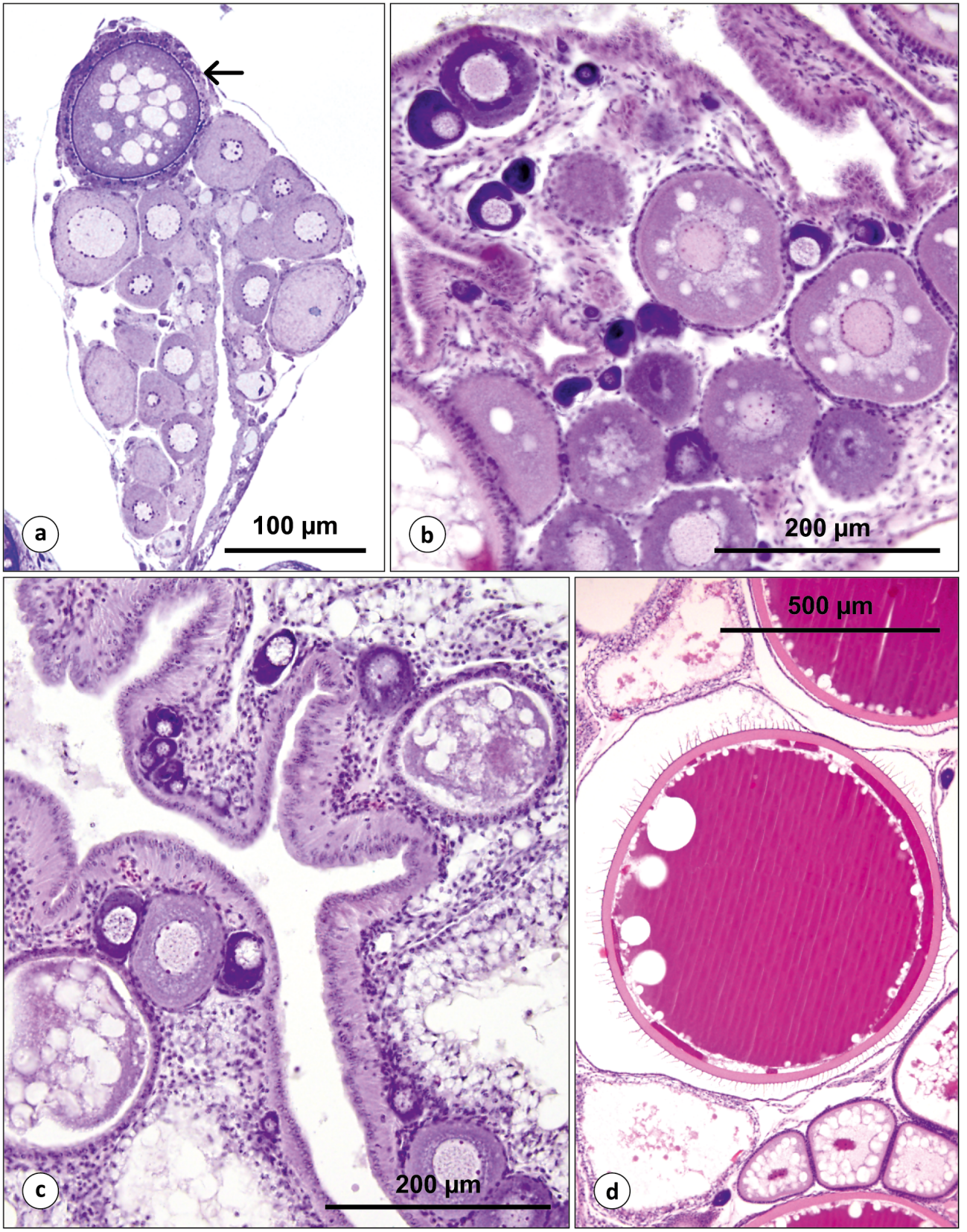

Fig. 33. Female gonads. (a) Longitudinal section of 11-day-old female with primary oocyte in the yolk globule stage of development (←) and multiple oogonia that differ in diameter depending on the stage of their development. (b) Ovigerous lamella in ovary. Vitellogenesis is seen in three primary oocytes. (c) Part of female gonads demonstrating asynchronous oogenesis, and oviduct. (d) Mature oocyte prepared for spawning. Adult NF (a, b, c), adult NE (d).

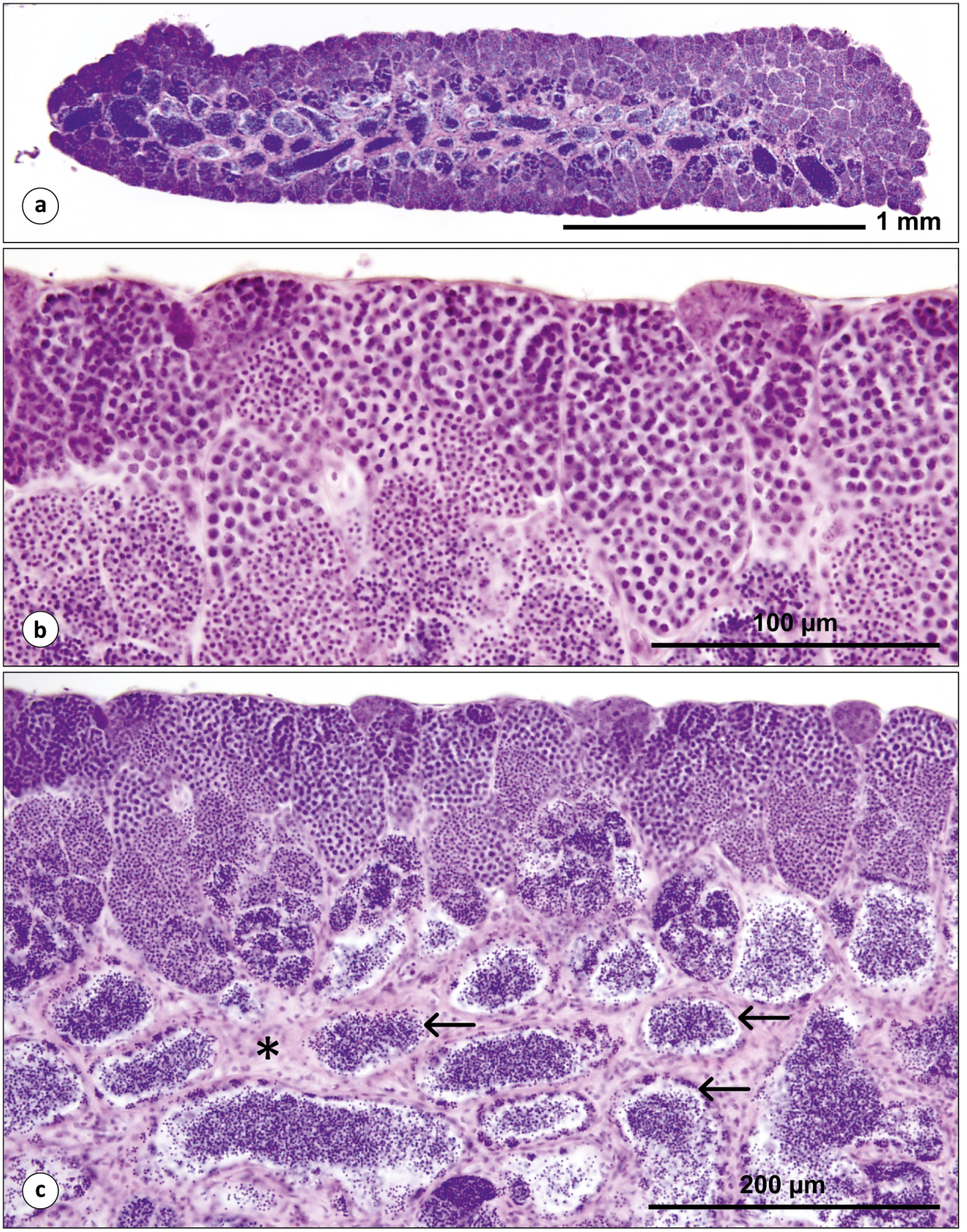

Fig. 34. Male gonads. (a) An overview of longitudinally sectioned testis that shows zonal architecture with subcapsular seminiferous lobules and centrally located tubules containing darkly stained mature spermatozoa. (b) Detail of testis periphery with spermatogonia of various sizes and primary and secondary spermatocytes. (c) Central part of male gonad that contains tubules with spermatids and mature spermatozoa (←) is rich in interstitial connective tissue (*). Adult NF.

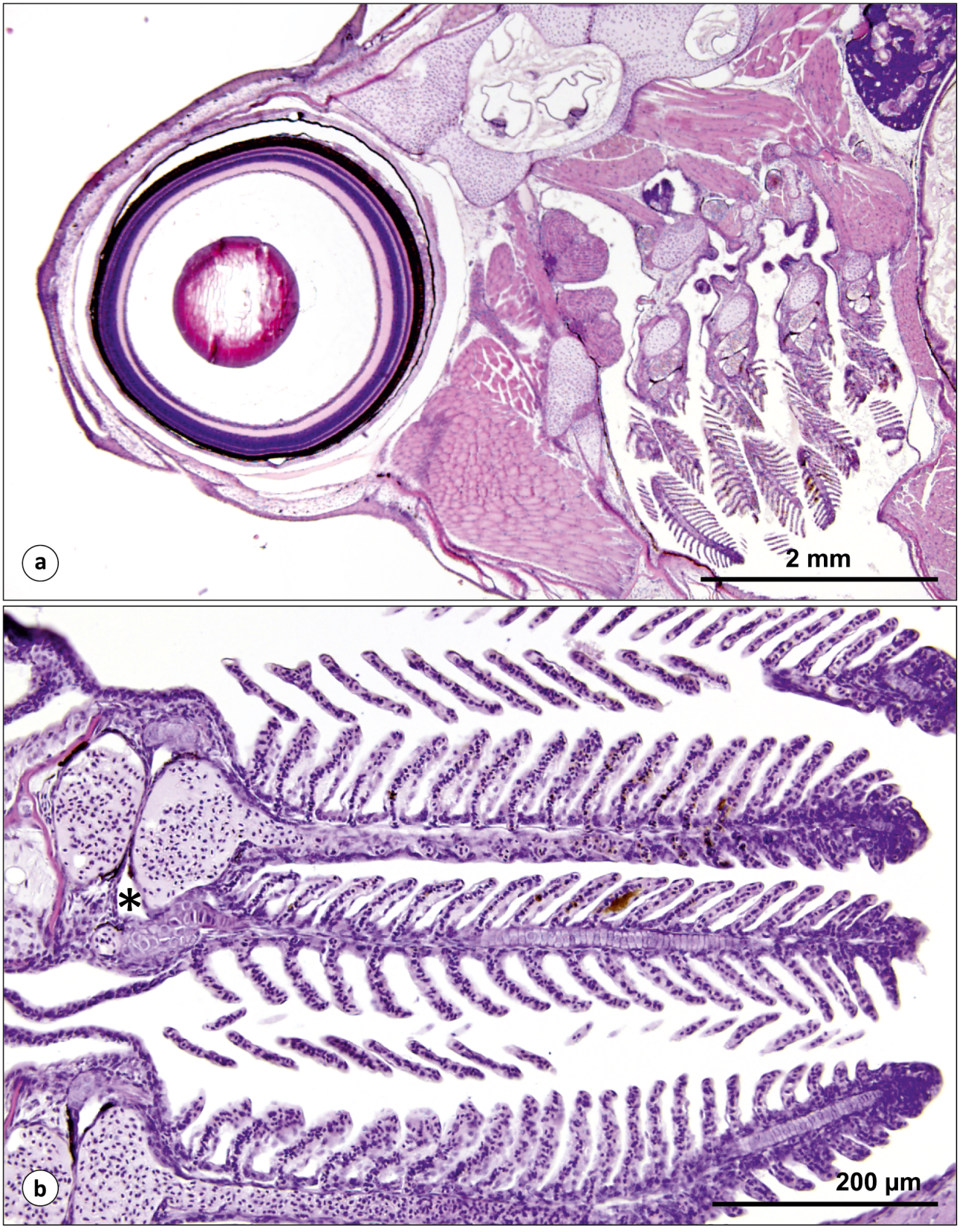

Fig. 35. Gills. (a) An overview of topology shows four gill arches in a parasagittal section through anterior part of NF body. (b) Longitudinal sections through gill filaments with secondary lamellae projecting to both sides of filament axes. Gill filament cartilage is absent at the level of sectioning, afferent and efferent blood vessels are seen at the basis of gill filaments (*). Adult NF.

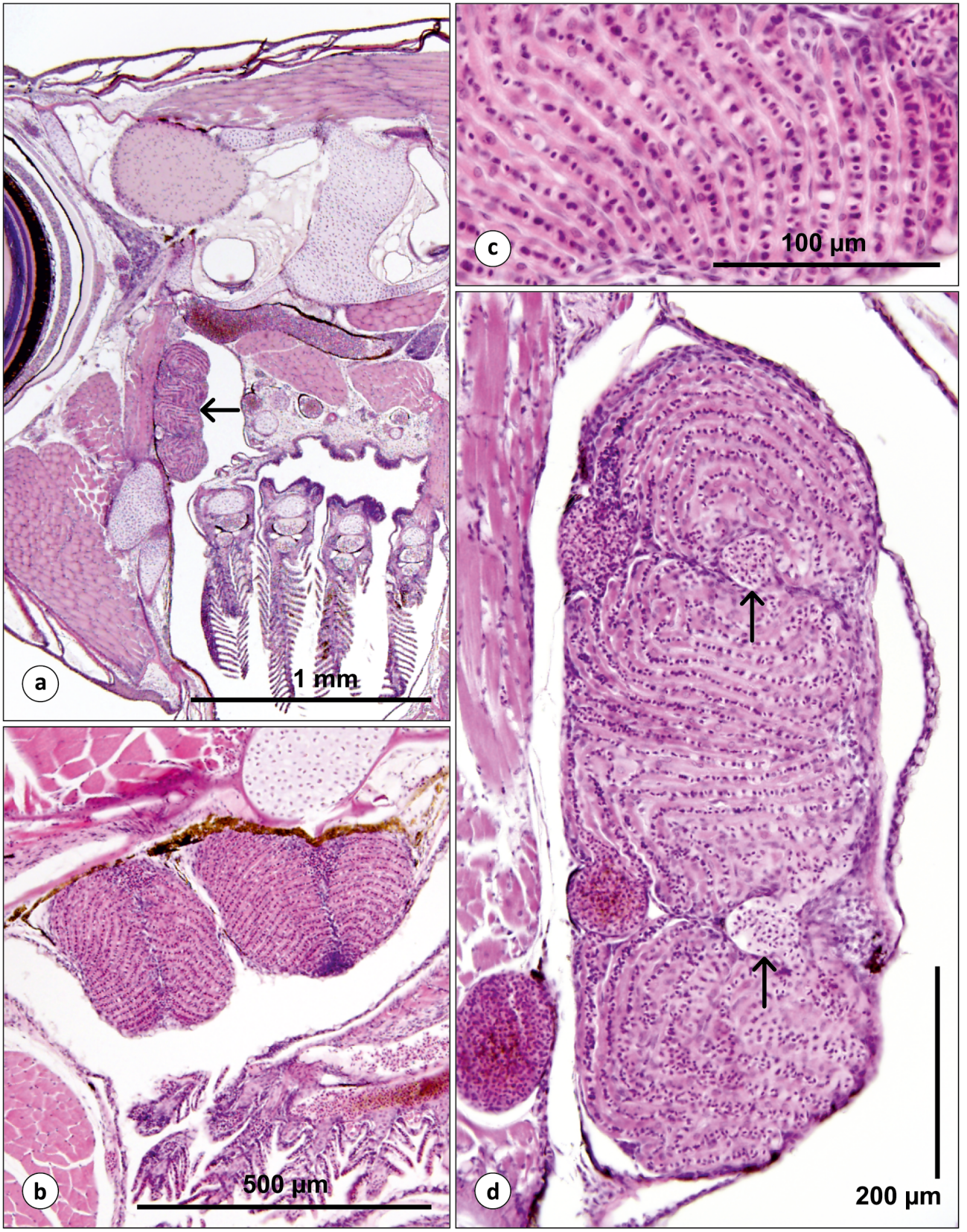

Fig. 36. Pseudobranch. (a) Parasagittal section through anterior part of NF body shows mutual position of pseudobranch (←), gills and other organs. (b) Two lobes of pseudobranch with parallel arranged blood capillaries. (c) Pseudobranch capillaries in detail. Rows of pilaster and epithelial cells resemble secondary lamellae of gill. (d) An overview of pseudobranch with blood vessels marked (↑). Functions of this organ are still to be defined in full. Adult NF.

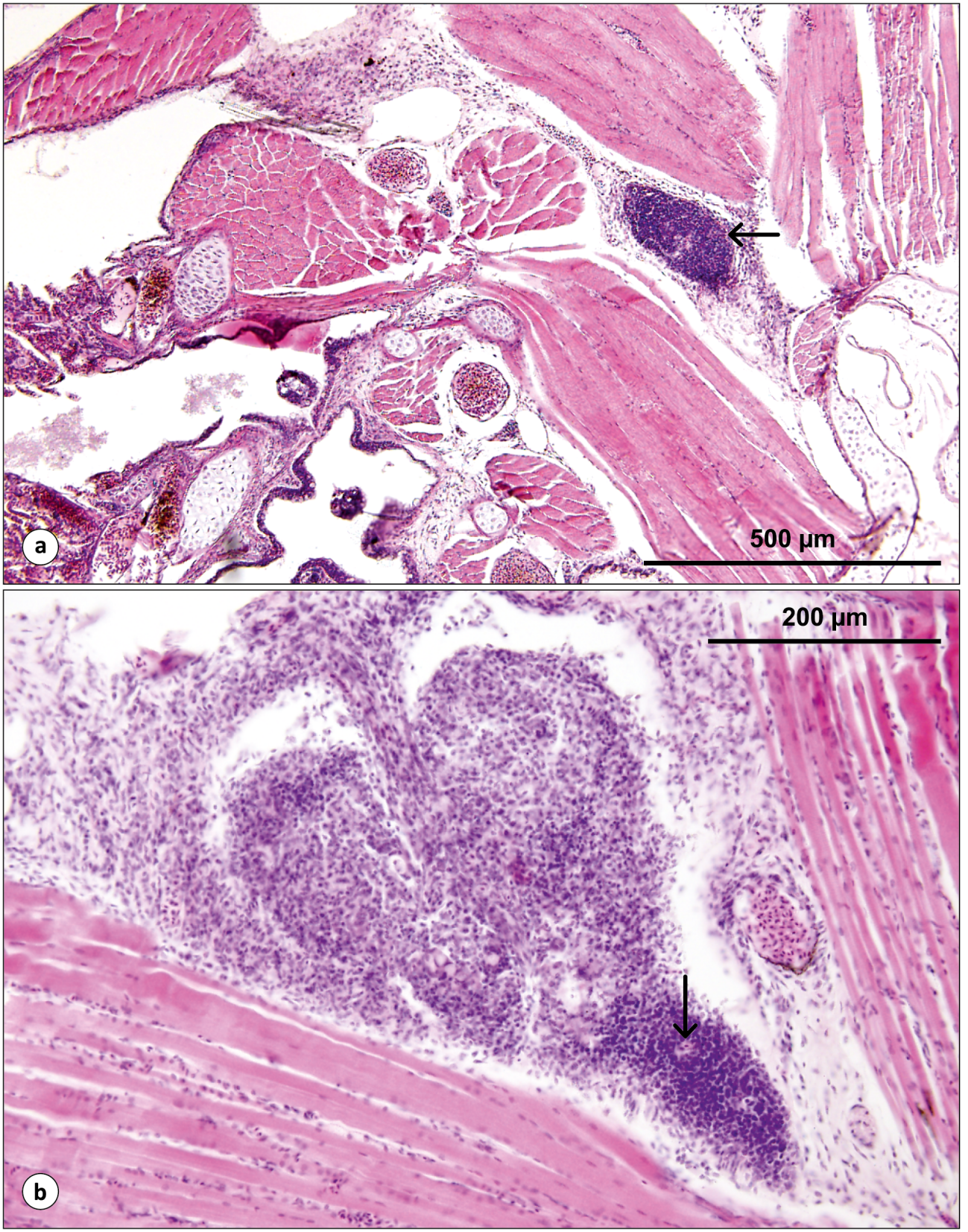

Fig. 37. Thymus. (a) Thymus (←), a paired lymphoid organ, is shown in parasagittal plane of sectioning as an aggregate of basophilic cells situated close to dorsal part of gill cavity. (b) Aggregate of basophilic lymphoid tissue composed of thymocytes resembling small lymphocytes is the site of differentiation of lymphocytes involved in cell-mediated immunity. Although not described in cyprinodontids, Hassall's-like structures (↓) are suspected among thymocytes. Adult NF.

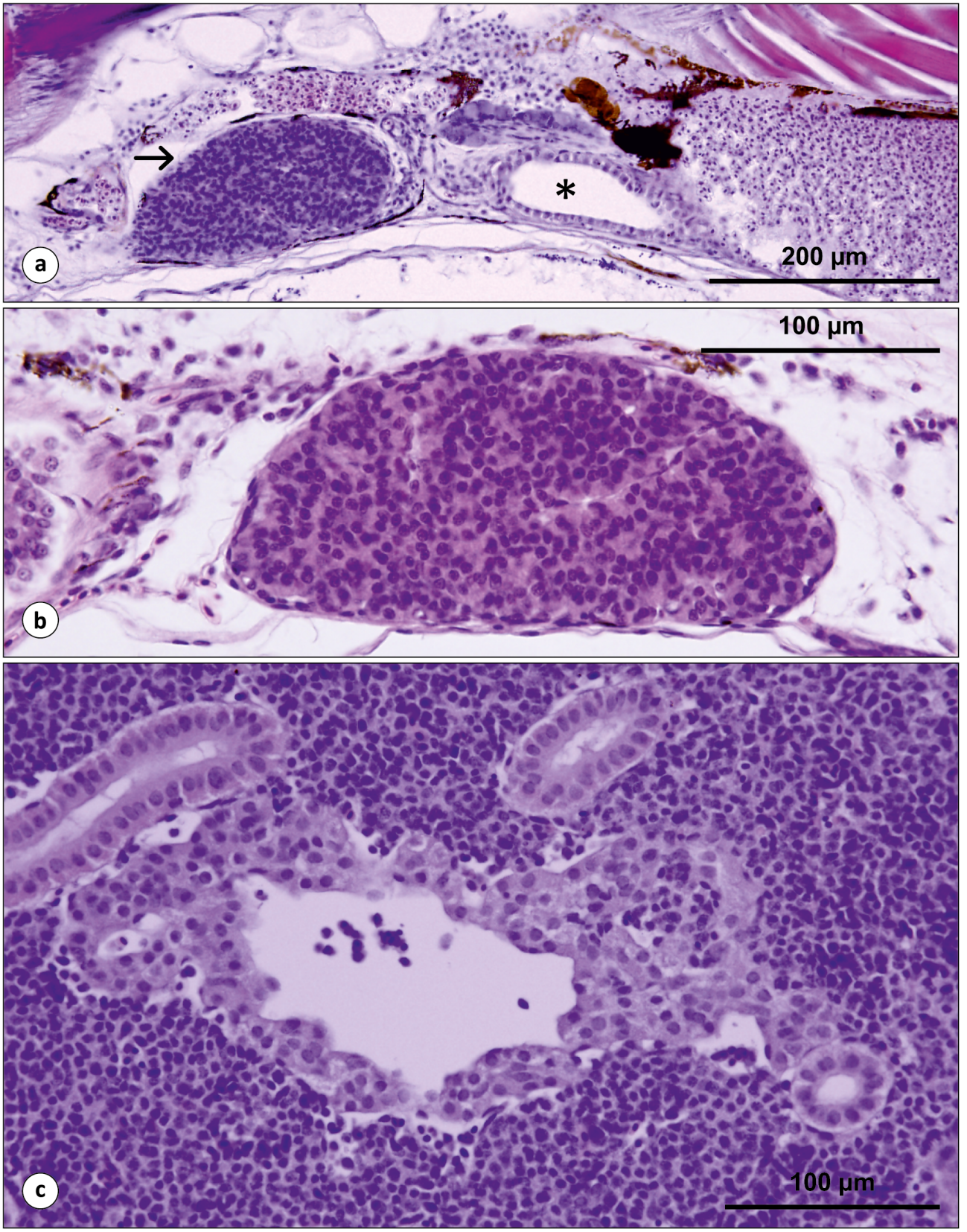

Fig. 38. Tissues with endocrine activity. (a) Stannius body (→), reported as organ involved in calcium homeostasis of teleosts, in dorso-caudal part of abdominal cavity, near to collecting/urinary duct (*). (b) Oval cluster of uniform glandular cells of Stannius body in detail. (c) Interrenal tissue considered homologue to the adrenal cortex of mammals is concentrated around posterior cardinal vein (this section: level of transition of head to trunk kidney). NP (a), NF (b, c).

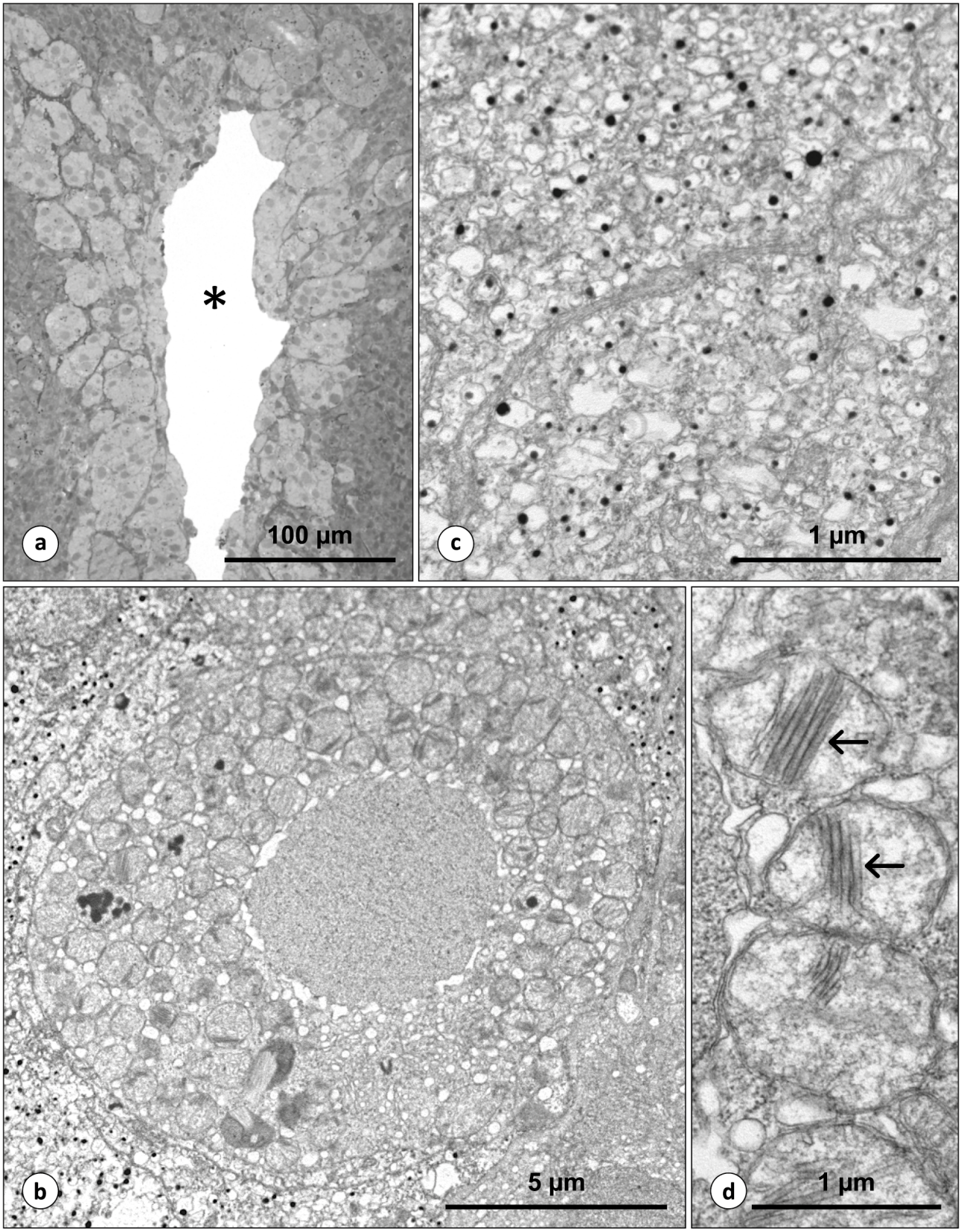

Fig. 39. Ultrastructure of interrenal tissue has not been fully explored yet, however, similarities with mammalian adrenal gland medulla are obvious. (a) Interrenal tissue concentrated around posterior cardinal vein (*) in semi-thin section. (b) Interrenal cell of unknown endocrine function. (c) Cell cytoplasm closely resembling that of norepinephrine-secreting cells, identified by dense core vesicles. (d) Mitochondria of (b) cell with prominent bundles of tubular cristae (←). NF.

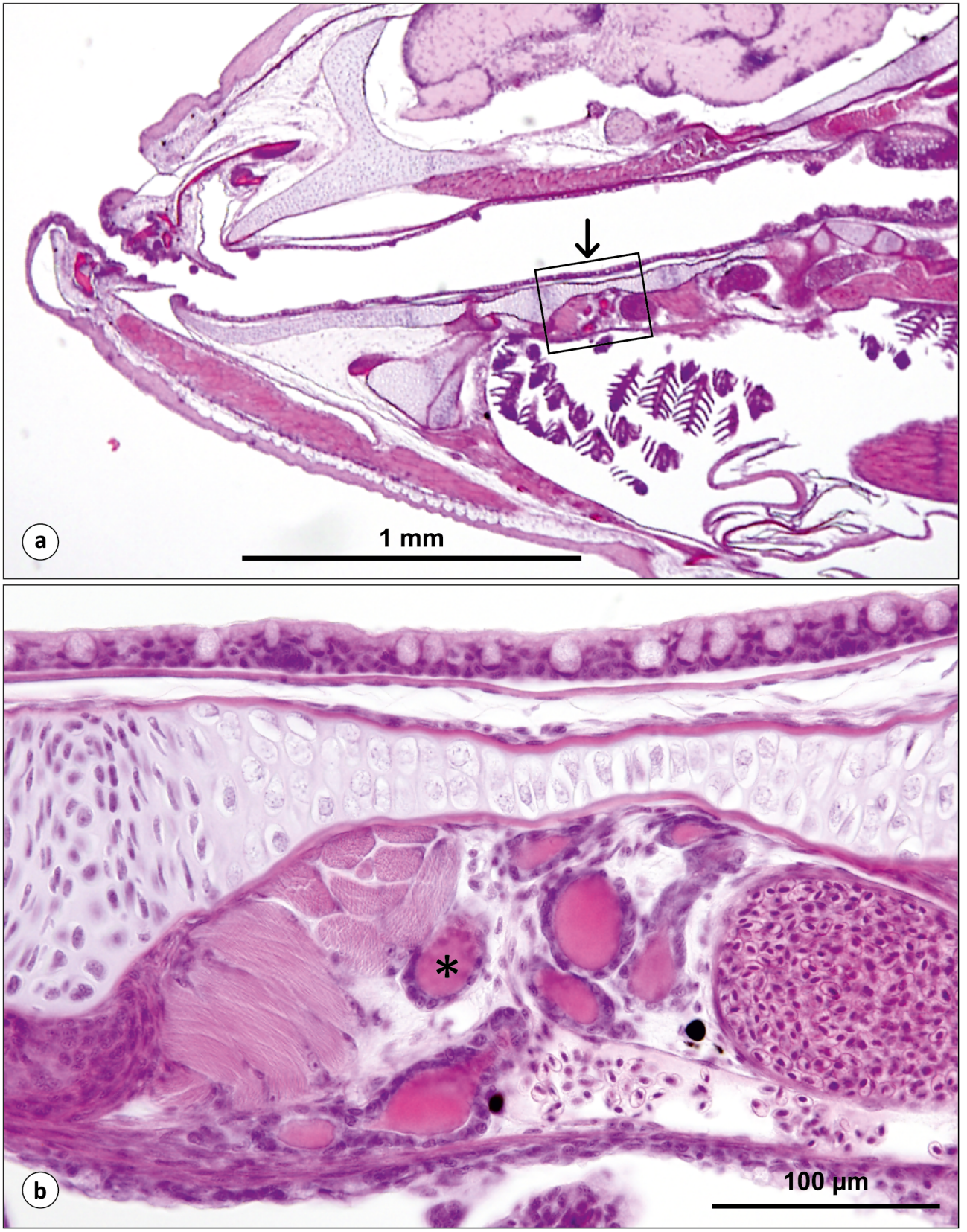

Fig. 40. Thyroid gland. (a) Thyroid follicles, structural and functional units of thyroid gland, were found in subpharyngeal and even more anterior location (↓). (b) Detail corresponding to the area marked in (a)**.** Follicles (*) filled with strongly eosinophilic colloid are diffusely scattered alongside blood vessels and are lined by simple cuboidal epithelium. Heterotopic follicles known to be localized in the kidney of many teleosts were not found in *Nothobranchius* fishes. NE (a, b).